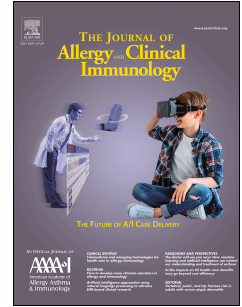


Journal Pre-proof



IL-33 Signaling in Sensory Neurons Promotes Dry Skin Itch

Anna M. Trier, B.A., Madison R. Mack, Ph.D., Avery Fredman, Masato Tamari, M.D. Ph.D., Aaron M. Ver Heul, M.D. Ph.D., Yonghui Zhao, Ph.D., Changxiong J. Guo, B.A., Oshri Avraham, Ph.D., Zachary K. Ford, Ph.D., Landon K. Oetjen, M.D. Ph.D., Jing Feng, Ph.D., Carina Dehner, M.D. Ph.D., Dean Coble, Ph.D., Asima Badic, RMA, Satoru Joshita, M.D. Ph.D., Masato Kubo, Ph.D., Robert W. Gereau, IV, Ph.D., Jennifer Alexander-Brett, M.D. Ph.D., Valeria Cavalli, Ph.D., Steve Davidson, Ph.D., Hongzhen Hu, Ph.D., Qin Liu, Ph.D., Brian S. Kim, M.D. M.T.R.

PII: S0091-6749(21)01405-6

DOI: <https://doi.org/10.1016/j.jaci.2021.09.014>

Reference: YMAI 15278

To appear in: *Journal of Allergy and Clinical Immunology*

Received Date: 2 May 2021

Revised Date: 27 August 2021

Accepted Date: 8 September 2021

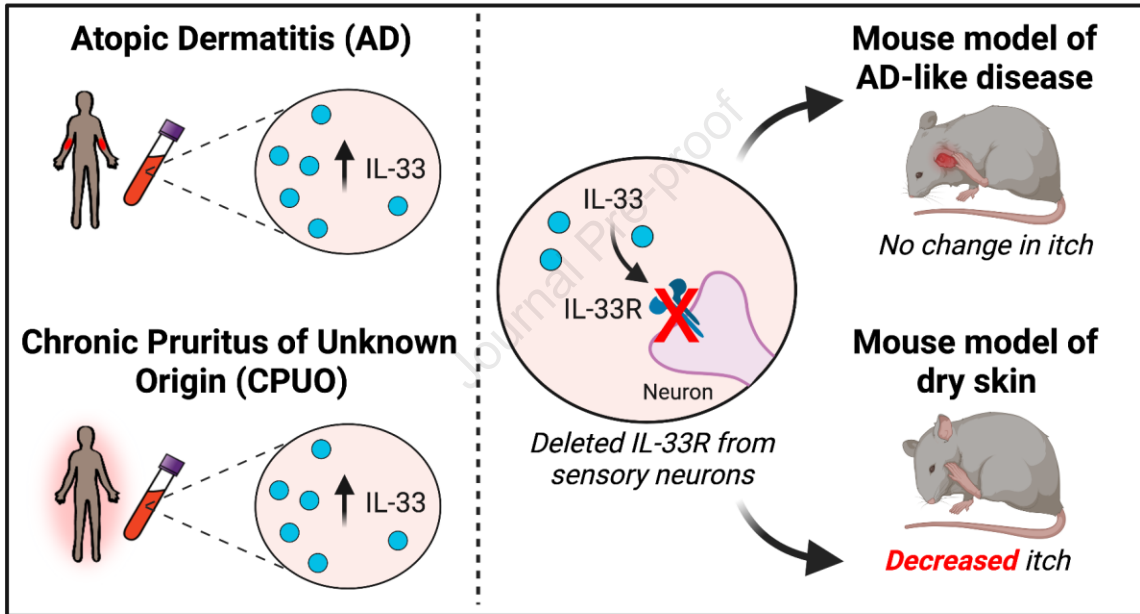
Please cite this article as: Trier AM, Mack MR, Fredman A, Tamari M, Ver Heul AM, Zhao Y, Guo CJ, Avraham O, Ford ZK, Oetjen LK, Feng J, Dehner C, Coble D, Badic A, Joshita S, Kubo M, Gereau IV RW, Alexander-Brett J, Cavalli V, Davidson S, Hu H, Liu Q, Kim BS, IL-33 Signaling in Sensory Neurons Promotes Dry Skin Itch, *Journal of Allergy and Clinical Immunology* (2021), doi: <https://doi.org/10.1016/j.jaci.2021.09.014>.

This is a PDF file of an article that has undergone enhancements after acceptance, such as the addition of a cover page and metadata, and formatting for readability, but it is not yet the definitive version of record. This version will undergo additional copyediting, typesetting and review before it is published in its final form, but we are providing this version to give early visibility of the article. Please note that, during the production process, errors may be discovered which could affect the content, and all legal disclaimers that apply to the journal pertain.

© 2021 Published by Elsevier Inc. on behalf of the American Academy of Allergy, Asthma & Immunology.



Neuronal IL-33R is necessary for dry skin itch, but not for itch in atopic dermatitis



IL-33 Signaling in Sensory Neurons Promotes Dry Skin Itch

Anna M. Trier B.A.^{1,2}, Madison R. Mack Ph.D.^{1,2,14}, Avery Fredman^{1,2}, Masato Tamari M.D. Ph.D.^{1,2}, Aaron M. Ver Heul M.D. Ph.D.^{1,3}, Yonghui Zhao Ph.D.^{1,4}, Changxiong J. Guo B.A.^{1,4}, Oshri Avraham Ph.D.⁵, Zachary K. Ford Ph.D.⁶, Landon K. Oetjen M.D. Ph.D.^{1,2}, Jing Feng Ph.D.^{1,4}, Carina Dehner M.D. Ph.D.², Dean Coble Ph.D.⁷, Asima Badic RMA^{1,2}, Satoru Joshita M.D. Ph.D.⁸, Masato Kubo Ph.D.^{9,10}, Robert W. Gereau IV Ph.D.^{4,5,11}, Jennifer Alexander-Brett M.D. Ph.D.¹², Valeria Cavalli Ph.D.⁵, Steve Davidson Ph.D.⁶, Hongzhen Hu Ph.D.^{1,4}, Qin Liu Ph.D.^{1,4} and Brian S. Kim M.D. M.T.R.^{1,2,4,13,*}

¹Center for the Study of Itch & Sensory Disorders, Washington University School of Medicine, St. Louis, MO 63110, USA.

²Division of Dermatology, Department of Medicine, Washington University School of Medicine, St. Louis, MO 63110, USA.

³Division of Allergy and Immunology, Department of Medicine, Washington University School of Medicine, St. Louis, MO 63110, USA.

⁴Department of Anesthesiology, Department of Medicine, Washington University School of Medicine, St. Louis, MO 63110, USA.

⁵Department of Neuroscience, Washington University School of Medicine, St. Louis, MO 63110, USA.

⁶Department of Anesthesiology and Neuroscience Program, University of Cincinnati College of Medicine, Cincinnati, OH 45267, USA.

⁷Division of Biostatistics, Washington University School of Medicine, St. Louis, MO 63110, USA.

⁸Division of Gastroenterology, Department of Medicine, Shinshu University School of Medicine, 3-1-1 Asahi, Matsumoto, Nagano, 390-8621, Japan.

⁹Laboratory of Cytokine Regulation, Center for Integrative Medical Science (IMS), RIKEN Yokohama Institute, Yokohama, Kanagawa, Japan.

¹⁰Division of Molecular Pathology, Research Institute for Biomedical Science, Tokyo University of Science, Noda 278-0022, Chiba Prefecture, Japan.

¹¹Washington University Pain Center, Washington University School of Medicine, St. Louis, MO 63110, USA.

¹²Division of Pulmonary and Critical Care, Department of Medicine, Washington University School of Medicine, St. Louis, MO 63110, USA.

¹³Department of Pathology and Immunology, Washington University School of Medicine, St. Louis, MO 63110, USA.

¹⁴Present address: Immunology and Inflammation Therapeutic Area, Sanofi, Cambridge, MA 02139, USA

*Corresponding Author

Corresponding Author

Brian S. Kim

Phone: (314) 273-1376

Email: briankim@wustl.edu

Address: 660 S. Euclid Avenue - Box 8123, St. Louis, MO 63110, USA

52 Funding statement:

53 Research in the Kim lab is supported by the Celgene Corporation, Doris Duke Charitable
54 Foundation, LEO Pharma, and NIAMS (K08AR065577, R01AR070116, R01AR077007, and
55 R21AI167047) (to B.S.K.). A.M.T. and M.R.M. are supported by NIAID (T32AI007163). A.M.T.
56 and L.K.O. are supported by NHLBI (T32HL007317). A.M.T. is supported by NIAID
57 (F30AI154912). Research in the Gereau lab involving human DRG research is supported by
58 NINDS (R01NS042595) (to R.W.G.). Research in the Alexander-Brett lab is supported by
59 NHLBI (R01HL152245) and the Burroughs Wellcome Fund (1014685) (to J.A.B). Research in
60 the Cavalli lab is supported by the McDonnell Center for Cellular and Molecular Neurobiology
61 and NINDS (R01NS111719) (to V.C.). O.A. is supported by the post-doctoral fellowship from
62 The McDonnell Center for Cellular and Molecular Neurobiology. Research in the Davidson lab is
63 supported by NINDS (RF1NS113881) (to S.D.). Research in the Hu lab is supported by NIAAA
64 (R01AA027065), NIAMS (R01AR077183), and NIDDK (R01DK103901) (to H.H.). Additional
65 support was provided by the Washington University School of Medicine Digestive Disease
66 Research Core Center (NIDDK, P30DK052574). Research in the Liu lab is supported by NIAID
67 (R01AI125743), Brain Research Foundation Fay / Frank Seed Grant, and Pew Scholar Award
68 (to Q.L.). Support with flow cytometry and Luminex was provided by the Bursky Center for
69 Human Immunology & Immunotherapy Programs at Washington University, Immunomonitoring
70 Laboratory (IML). The IML is a shared resource of the Alvin J. Siteman Cancer Center
71 (Washington University School of Medicine and Barnes-Jewish Hospital in St. Louis), which is
72 supported in part by NCI (P30CA091842).

73

74 Disclosure statement:

75 B.S.K. has served as a consultant for: AbbVie, Almirall, AstraZeneca, Cara Therapeutics,
76 Daewoong Pharmaceutical, Incyte Corporation, LEO Pharma, Lily, Maruho, OM Pharma, Pfizer,
77 and Third Rock Ventures. He has also participated on the advisory board for: Almirall,

78 Boehringer Ingelheim, Cara Therapeutics, Kiniksa Pharmaceuticals, Regeneron
79 Pharmaceuticals, Sanofi Genzyme, and Trevi Therapeutics. Additionally, he is a stockholder of
80 Locus Biosciences. He also serves on the scientific advisory board for Abrax Japan, Granular
81 Therapeutics, Recens Medical, National Eczema Association, and Cell Reports Medicine. All
82 other authors declare they have no relevant conflicts of interest.

83

84 **Abstract**

85

86 Background: Chronic pruritus, or itch, is common and debilitating, but the neuro-immune
87 mechanisms that drive chronic itch are only starting to be elucidated. Recent studies
88 demonstrate that the IL-33 receptor (IL-33R) is expressed by sensory neurons. However,
89 whether sensory neuron-restricted activity of IL-33 is necessary for chronic itch remains poorly
90 understood.

91

92 Objectives: We sought to determine if IL-33 signaling in sensory neurons is critical for the
93 development of chronic itch in two divergent pruritic disease models.

94

95 Methods: Plasma levels of IL-33 were assessed in patients with atopic dermatitis (AD) and
96 chronic pruritus of unknown origin (CPUO). Mice were generated to conditionally delete IL-33R
97 from sensory neurons. The contribution of neuronal IL-33R signaling to chronic itch
98 development was tested in mouse models that recapitulate key pathologic features of AD and
99 CPUO, respectively.

100

101 Results: IL-33 was elevated in both AD and CPUO as well as their respective mouse models.

102 While neuron-restricted IL-33R signaling was dispensable for itch in AD-like disease, it was

103 required for the development of dry skin itch in a mouse model that mirrors key aspects of
104 CPUO pathology.

105
106 Conclusion: These data highlight how IL-33 may be a predominant mediator of itch in certain
107 contexts, depending on the tissue microenvironment. Further, this study provides insight for
108 future therapeutic strategies targeting the IL-33 pathway for chronic itch.

109 110 **Key Message**

- 111 • IL-33 is elevated in two divergent pruritic disease conditions and their respective models
- 112 • Signaling of the IL-33 receptor in sensory neurons is necessary for dry skin itch, but not
113 itch associated with atopic dermatitis-like disease

114 115 **Capsule Summary**

116 IL-33 signaling in sensory neurons drives chronic itch in dry skin with minimal inflammation and
117 is dispensable in AD-like disease. These findings provide insight on anti-IL-33 mAb therapies
118 currently in phase 2 clinical trials.

119 120 **Key Words**

121 Atopic dermatitis, chronic pruritus of unknown origin, dry skin, IL-33, itch, neuroimmunology,
122 pruriceptor, pruritogen

123 124 **Abbreviations**

125 Ab (antibody), AD (atopic dermatitis), AEW (acetone/ether plus water), bp (base pair), Cap
126 (Capsaicin), CPUO (chronic pruritus of unknown origin), CQ (chloroquine), DRG (dorsal root
127 ganglia), DT (diphtheria toxin), epidermis (Epi), EtOH (ethanol), HC (healthy control), His
128 (histamine), i.d. (intradermal), ILC2s (group 2 innate lymphoid cells), IL-33R (IL-33 receptor), i.p.

129 (intraperitoneal), KCl (potassium chloride), LM (littermate), loxP (locus of X-over P1), mAb
130 (monoclonal antibody), MACS (magnetic-activated cell sorting), MasTRECK (mast cell-specific
131 enhancer-mediated toxin receptor-mediated conditional cell knockout), NS (no significance), rh
132 (recombinant human), rm (recombinant mouse), RNA-seq (RNA sequencing), stratum corneum
133 (SC), Veh (Vehicle), WT (wild-type)

134

135 **Introduction**

136

137 Chronic pruritus, or itch, is a debilitating, often intractable condition that causes a reduction in
138 quality of life similar to chronic pain and has a lifetime prevalence of up to 20%.^{1,2} Recent
139 studies have identified that various cytokines can function as itch-inducing factors, or
140 pruritogens, at the neuro-immune interface, and there is mounting interest in harnessing the
141 therapeutic potential of blocking these interactions.³

142

143 Epithelial cell-derived IL-33 is a potent amplifier of type 2 immune responses and is increasingly
144 implicated in itch, although the mechanisms remain unclear.⁴ It has recently been demonstrated
145 that the IL-33 receptor (IL-33R) is expressed in the dorsal root ganglia (DRG) and that IL-33 can
146 directly activate sensory neurons.^{5,6} However, whether IL-33R expression in sensory neurons is
147 specifically required for the development of chronic itch, and in what disease setting, remains
148 poorly defined.

149

150 **Results and Discussion**

151

152 IL-33 acts as an 'alarmin' by being rapidly released from damaged epithelial cells to initiate type
153 2 inflammation.⁴ In addition to immune cells, IL-33R is also expressed by sensory neurons.^{5,6}
154 We confirmed expression of IL-33R (ST2, *Il1rl1*) in mouse DRG (**Fig 1, A**) and, using calcium

155 imaging, found that IL-33 activated 2.1% of DRG neurons (**Fig 1, B and C**). Further, we found
156 that 52% and 63% of IL-33-responsive mouse DRG neurons also responded to histamine and
157 the TRPV1-agonist capsaicin, respectively (**Fig 1, D**). Similarly, we found IL-33R was expressed
158 by human DRG (**Fig 1, E**) and 6.6% of human DRG neurons were responsive to IL-33 (**Fig 1, F**
159 **and G**). Of these neurons, 60% also responded to capsaicin (**Fig 1, H**). Together these findings
160 suggest that IL-33 can directly activate sensory neurons.

161
162 A recent study demonstrated that IL-33R knockdown within the DRG compartment attenuates
163 itch in allergic contact dermatitis.⁵ While these findings suggest that neuronal IL-33R signaling
164 may be a critically important itch pathway, the DRG contains a diversity of other cell types. The
165 expression of IL-33R in the DRG, beyond sensory neurons, has yet to be fully assessed. To
166 address this, we analyzed a single cell RNA-seq dataset of naïve mouse DRG (**Fig 1, I**).⁷ We
167 found that *Il1rl1* was indeed expressed by another cell type: DRG macrophages (**Fig 1, J**).
168 Similarly, analysis of other neuronally expressed itch-associated cytokine receptors, such as
169 *Il4ra*,⁸ revealed expression across numerous cell types (**Fig 1, K**). Taken together, these data
170 underscore that targeted, lineage-specific approaches are likely required to determine the
171 precise contribution of a distinct cell type to itch development. Therefore, the consequence of
172 disrupting IL-33R signaling specifically in sensory neurons remains unknown.

173
174 We generated mice in which loxP sites were inserted into the *Il1rl1* gene locus (IL-33R^{fllox} mice)
175 (**Fig 2, A**) and crossed these mice onto the SNS^{Cre} mouse line,⁹ generating mice that
176 conditionally lack IL-33R in sensory neurons (IL-33R^{Δneuron} mice). We confirmed the selective
177 loss of *Il1rl1* in sensory neurons, and not immune cells, isolated from IL-33R^{Δneuron} mice (**Fig 2,**
178 **B**). These mice exhibited normal motor function (**Fig 2, C**), thermal pain behavior (**Fig 2, D**), and
179 acute itch response to the classical pruritogens histamine (**Fig 2, E**), chloroquine (**Fig 2, F**), and

180 serotonin (**Fig 2, G**), indicating the mice have no gross developmental motor or sensory
181 abnormalities.

182

183 Advances in our understanding of the mechanisms underlying chronic itch have largely drawn
184 from studying inflammatory skin disorders such as atopic dermatitis (AD). AD presents with
185 pruritic skin lesions driven by type 2 inflammation.¹⁰ Given the ability of IL-33 to promote type 2
186 inflammation,¹⁰ there is considerable interest in the therapeutic potential of anti-IL-33
187 monoclonal antibodies (mAbs) in AD.^{3,11} Several studies have found elevated levels of IL-33 in
188 both the skin and blood of patients with AD.^{10,12,13} In support, we found that patients with
189 moderate-to-severe AD (N = 11, 5.17 ± 1.37) had increased IL-33 in their plasma compared to
190 healthy control (HC) subjects (N = 11, 3.93 ± 1.20) (**Fig 3, A and B, Table E1**). We next utilized
191 a model of AD-like disease, where mice are treated with MC903 (**Fig E1, A**). MC903-treated
192 wild-type (WT) mice developed robust AD-like skin inflammation (**Fig 3, C**).⁸ Indeed, analyzing
193 our previously published RNA-seq dataset,⁸ we found increased expression of *Il33*, along with
194 transcripts for a number of other pruritogens, in the skin of MC903-treated WT mice compared
195 to controls (**Fig 3, D**). However, while it is well-known that IL-33 is dysregulated in both human
196 and murine AD-associated inflammation, whether IL-33 directly engages the sensory nervous
197 system to elicit itch remains unclear. When we induced AD-like disease in IL-33R^{Δneuron} mice,
198 there were no notable differences in clinical or histopathological presentation (**Fig 3, E**), ear
199 thickness (**Fig 3, F**), or scratching bouts (**Fig 3, G**) compared to littermate (LM) controls. Thus,
200 our findings suggest that neuronal IL-33R is dispensable for AD-like disease.

201

202 In AD-like skin, many putative pruritogens are upregulated (**Fig 3, D**) and may override the
203 contribution of IL-33 to itch. Thus, we next sought to test whether neuron-restricted IL-33R may
204 play a more important role in itch that arises in the absence of robust skin inflammation. Chronic
205 pruritus of unknown origin (CPUO) accounts for 10-40% of all chronic itch cases, is poorly

206 understood, and lacks effective therapies.^{1,14} While patients with AD present with scaly, raised
207 rashes (**Fig 4, A**), chronic itch in CPUO develops in the absence of overt cutaneous
208 inflammation. Additionally, CPUO disproportionately occurs in aged individuals.¹⁴ A key
209 pathogenic factor of CPUO is skin barrier dysfunction, which frequently manifests as dry skin
210 (**Fig 4, B**). The histopathology of CPUO often resembles control skin (**Fig 4, C**), while AD
211 lesional skin exhibits a number of characteristic inflammatory features including irregular
212 epidermal hyperplasia and robust dermal inflammatory infiltrate (**Fig 4, D**). In contrast, CPUO
213 pruritic skin generally exhibits a relatively normal epidermis and mild dermal infiltrate (**Fig 4, E**).
214 We found that patients with CPUO (N = 8, 6.22 ± 2.54) had significantly higher levels of IL-33
215 compared to HCs (N = 11, 3.93 ± 1.20) (**Fig 4, F and G, Table E1**). Thus, we hypothesized that
216 IL-33 may be a key factor in itch physiology associated with CPUO.

217
218 To examine the role of IL-33 in a disease model that recapitulates key pathological features of
219 CPUO, we utilized the acetone/ether plus water (AEW) mouse model (**Fig E1, B**). This model is
220 characterized by the development of dry skin (**Fig 5, A**) and other pathogenic changes that
221 mimic aged skin.^{15,16} We have previously utilized the AEW mouse model to identify novel
222 therapeutic approaches that led to proof-of-concept studies in CPUO.⁸ In contrast to other
223 mouse models of chronic itch, AEW-elicited itch develops in the absence of notable cutaneous
224 inflammation, similar to CPUO. Indeed, the frequency of cutaneous immune cells (**Fig 5, B**),
225 including mast cells (**Fig 5, C**) and group 2 innate lymphoid cells (ILC2s) (**Fig 5, D**), were
226 comparable between WT mice that were treated with AEW and water-only controls, despite
227 significantly increased itch behavior in AEW-treated mice (**Fig 5, E**). Notably, *Il33* was elevated
228 in the skin of AEW-treated mice compared to controls (**Fig 5, F**).¹⁷ Taken together, our findings
229 demonstrate that AEW-induced itch is associated with IL-33 dysregulation and minimal
230 cutaneous inflammation, similar to CPUO.

231

232 It was recently reported that global deficiency of IL-33 or IL-33R results in decreased AEW-
233 induced itch.¹⁸ However, how IL-33 drives the development of dry skin itch is poorly understood.
234 Indeed, whether IL-33 can promote itch through a mechanism independent of canonical immune
235 circuits remains unknown. Mast cells, and more recently basophils, have been implicated as key
236 mediators of itch.^{19–21} To test if these cell types contribute to dry skin itch, we employed
237 MasTRECK mice, which allow for diphtheria toxin (DT)-mediated depletion of mast cells and
238 basophils (**Fig E2**). However, AEW-induced scratching bouts were comparable between DT-
239 treated LM control and MasTRECK mice (**Fig 5, G**). IL-33 also potently activates both ILC2s
240 and T cells to modulate the skin immune responses.⁴ However, we found no difference in itch
241 between AEW-treated lymphocyte-deficient *Rag2/Il2rg*^{-/-} mice and controls (**Fig 5, H**). Finally, we
242 generated mice that conditionally lack IL-33R in immune cells by crossing the IL-33R^{flox} mice
243 with the *Vav*^{Cre} line (IL-33R^{Δimmune}). Following AEW-treatment, there was no difference in the
244 number of scratching bouts between LM control and IL-33^{Δimmune} mice (**Fig 5, I**). Collectively,
245 these data suggest that immune cells are largely dispensable for the induction of dry skin itch
246 and instead implicate sensory neurons as the potential primary target of IL-33 for itch
247 development.

248
249 To test the hypothesis that neuronal IL-33R regulates dry skin itch, we utilized the IL-33R^{Δneuron}
250 mice. Strikingly, AEW-treated IL-33R^{Δneuron} mice demonstrated significantly attenuated itch
251 behavior compared to LM controls (**Fig 5, J**). Despite the requirement of neuronal IL-33R for dry
252 skin itch, IL-33 alone was not sufficient to induce robust acute itch responses (**Fig 5, K**), similar
253 to prior reports.⁵ This led us to hypothesize that IL-33 may instead sensitize sensory neurons.
254 Indeed, it has been shown that AEW-treated mice exhibit enhanced responsiveness to
255 exogenous pruritogens like chloroquine (CQ).^{22,23} However, the mechanisms underlying these
256 observations are not well understood. Using calcium imaging, in a proof-of-concept experiment,
257 we found that IL-33 treatment of DRG neurons increased the number of cells responding to CQ

258 **(Fig 5, L and M)**. Thus, although CQ is not a native endogenous pruritogen in dry skin, these
259 studies represent one example by which IL-33 may amplify responses to pruritogens in order to
260 promote chronic itch. Future studies will be required to determine the precise molecular
261 mechanisms by which IL-33 may enhance itch in this manner.

262
263 Our findings suggest that neuron-restricted IL-33R signaling is a critical regulator of itch that
264 arises in the setting of dry skin, independent of immune cells. Furthermore, our findings are
265 consistent with prior studies demonstrating that IL-33 may be dispensable for the development
266 of AD-like disease.^{24,25} Together, these findings may help explain why anti-IL-33 mAbs (e.g.
267 etokimab) have failed to meet their primary endpoints or have been discontinued following
268 recent phase 2 clinical trials in AD (NCT03533751, NCT03736967). In contrast, IL-33 may be an
269 important therapeutic target in dry skin itch and CPUO.

270

271 **Acknowledgments:**

272 We would like to thank the LifeCenter, Cincinnati and the generosity of the donors and their
273 families. We also thank Diane Bender for help with the Luminex analysis. We thank Dr. Rohini
274 Kuner for donating the SNS^{Cre} mouse line and Dr. Siji Nishino for providing the MastRECK
275 mouse line. We additionally thank Dr. Douglas Lopes for his technical guidance. Figures created
276 in part with Biorender.com.

277

278 **References:**

279

- 280 1. Weisshaar E, Dalgard F. Epidemiology of itch: Adding to the burden of skin morbidity.
281 Acta Derm Venereol. 2009;89:339–50.
- 282 2. Kini SP. The Impact of Pruritus on Quality of Life. Arch Dermatol. 2011;147:1153.
- 283 3. Wang F, Kim BS. Itch: A Paradigm of Neuroimmune Crosstalk. Immunity. 2020;52:753–
284 66.
- 285 4. Chan BCL, Lam CWK, Tam LS, Wong CK. IL33: Roles in allergic inflammation and
286 therapeutic perspectives. Front Immunol. 2019;10:1–11.
- 287 5. Liu B, Tai Y, Achanta S, Kaelberer MM, Caceres AI, Shao X, et al. IL-33/ST2 signaling
288 excites sensory neurons and mediates itch response in a mouse model of poison ivy
289 contact allergy. Proc Natl Acad Sci U S A. 2016;113:E7572–9.

- 290 6. Huang J, Gandini MA, Chen L, M'Dahoma S, Stemkowski PL, Chung H, et al.
291 Hyperactivity of Innate Immunity Triggers Pain via TLR2-IL-33-Mediated Neuroimmune
292 Crosstalk. *Cell Rep.* 2020;33:108233.
- 293 7. Avraham O, Feng R, Ewan EE, Zhao G, Cavalli V. Profiling sensory neuron
294 microenvironment after peripheral and central axon injury reveals key pathways for axon
295 regeneration. *bioRxiv.* 2020; doi:10.1101/2020.11.25.398537
- 296 8. Oetjen LK, Mack MR, Feng J, Whelan TM, Niu H, Guo CJ, et al. Sensory Neurons Co-opt
297 Classical Immune Signaling Pathways to Mediate Chronic Itch. *Cell.* 2017;171:217-
298 228.e13.
- 299 9. Agarwal N, Offermanns S, Kuner R. Conditional gene deletion in primary nociceptive
300 neurons of trigeminal ganglia and dorsal root ganglia. *Genesis.* 2004;38:122–9.
- 301 10. Imai Y. Interleukin-33 in atopic dermatitis. *J Dermatol Sci.* 2019;96:2–7.
- 302 11. Peng G, Mu Z, Cui L, Liu P, Wang Y, Wu W, et al. Anti-IL-33 Antibody Has a Therapeutic
303 Effect in an Atopic Dermatitis Murine Model Induced by 2, 4-Dinitrochlorobenzene.
304 *Inflammation.* 2018;41:154–63.
- 305 12. Nakamura N, Tamagawa-Mineoka R, Yasuike R, Masuda K, Matsunaka H, Murakami Y,
306 et al. Stratum corneum interleukin-33 expressions correlate with the degree of
307 lichenification and pruritus in atopic dermatitis lesions. *Clin Immunol.* 2019;201:1–3.
- 308 13. Tamagawa-Mineoka R, Okuzawa Y, Masuda K, Katoh N. Increased serum levels of
309 interleukin 33 in patients with atopic dermatitis. *J Am Acad Dermatol.* 2014;70:882–8.
- 310 14. Kim BS, Berger TG, Yosipovitch G. Chronic pruritus of unknown origin (CPUO): Uniform
311 nomenclature and diagnosis as a pathway to standardized understanding and treatment.
312 *J Am Acad Dermatol.* 2019;81:1223–4.
- 313 15. Miyamoto T, Nojima H, Shinkado T, Nakahashi T, Kuraishi Y. Itch-Associated Response
314 Induced by Experimental Dry Skin in Mice. *Jpn J Pharmacol.* 2002;88:285–92.
- 315 16. Feng F, Luo J, Yang P, Du J, Kim B, Hu H. Piezo2 channel-Merkel cell signaling
316 modulates the conversion of touch to itch. *Science (80).* 2018;360:530–3.
- 317 17. Wilson SR, Nelson AM, Batia L, Morita T, Estandian D, Owens DM, et al. The Ion
318 Channel TRPA1 Is Required for Chronic Itch. *J Neurosci.* 2013;33:9283–94.
- 319 18. Du L, Hu X, Yang W, Yasheng H, Liu S, Zhang W, et al. Spinal IL-33/ST2 signaling
320 mediates chronic itch in mice through the astrocytic JAK2-STAT3 cascade. *Glia.*
321 2019;67:1680–93.
- 322 19. Solinski HJ, Kriegbaum MC, Tseng PY, Earnest TW, Gu X, Barik A, et al. Nppb Neurons
323 Are Sensors of Mast Cell-Induced Itch. *Cell Rep.* 2019;26:3561-3573.e4.
- 324 20. Meixiong J, Anderson M, Limjunyawong N, Sabbagh MF, Hu E, Mack MR, et al.
325 Activation of Mast-Cell-Expressed Mas-Related G-Protein-Coupled Receptors Drives
326 Non-histaminergic Itch. *Immunity.* 2019;50:1163-1171.e5.
- 327 21. Wang F, Trier AM, Li F, Kim S, Chen Z, Chai JN, et al. A basophil-neuronal axis
328 promotes itch. *Cell.* 2021;184:422-440.e17.
- 329 22. Shi H, Yu G, Geng X, Gu L, Yang N, Wang C, et al. MrgprA3 shows sensitization to
330 chloroquine in an acetone-ether-water mice model. *Neuroreport.* 2017;28:1127–33.
- 331 23. Valtcheva M, Samineni V, Golden J, Gereau R, Davidson S. Enhanced non-peptidergic
332 intraepidermal fiber density and an expanded subset of chloroquine-responsive trigeminal
333 neurons in a mouse model of dry skin itch. *J Pain.* 2015;16:346–56.
- 334 24. Kim BS, Siracusa MC, Saenz SA, Noti M, Monticelli LA, Sonnenberg GF, et al. TSLP
335 Elicits IL-33-Independent Innate Lymphoid Cell Responses to Promote Skin
336 Inflammation. *Sci Transl Med.* 2013;5:170ra16.
- 337 25. Pietka W, Sundnes O, Hammarström C, Zucknick M, Khnykin D, Haraldsen G. Lack of
338 interleukin-33 and its receptor does not prevent calcipotriol-induced atopic dermatitis-like
339 inflammation in mice. *Sci Rep.* 2020;10:6451.
- 340

341
 342 **Figure 1: Mouse and human DRG express IL-33R.** (A) Gel of *Il1rl1* RT-PCR product from
 343 dorsal root ganglia (DRG) isolated from one wild-type (WT) mouse. Representative of three
 344 mice. (B) Representative calcium imaging trace of mouse DRG neuron in response to vehicle
 345 (Veh), recombinant mouse (rm)IL-33, capsaicin (Cap), and potassium chloride (KCl). (C)
 346 Percent of rmIL-33-, histamine (His)-, and Cap-responsive DRG neurons out of all KCl-
 347 responsive DRG neurons. (D) Venn diagrams of overlapping responses between IL-33-
 348 responsive (IL-33⁺) and Cap-responsive (Cap⁺) or His-responsive (His⁺) neurons. (B-D) n > 900
 349 neurons from at least 4 WT mice (6 combined experiments). (E) Gel of *IL1RL1* RT-PCR product
 350 from DRG isolated from one human donor. Representative of three donors. *Ladder has been
 351 previously published in Oetjen et al.⁸ (F) Representative calcium imaging trace of human DRG
 352 neuron in response to Veh, recombinant human (rh)IL-33, Cap, and KCl. (G) Percent of rhIL-33-
 353 and Cap-responsive DRG neurons out of all KCl-responsive DRG neurons. (H) Venn diagrams
 354 of overlapping responses between IL-33⁺ and Cap⁺ neurons. (F-H) N > 200 neurons from 2
 355 human subjects (2 combined experiments). (I) t-SNE plot of single cell RNA-seq of mouse DRG
 356 colored by cell populations. Violin plots of (J) *Il1rl1* and (K) *Il4ra* gene expression. Full dataset in
 357 Avraham et al.⁷

358

359 **Figure 2: Generation of IL-33R conditional deletion mice** (A) Map of *Il1rl1* conditional knock-
 360 out allele. blue triangles, loxP sites; gray boxes, exons; red box, conditionally deleted region. (B)
 361 Expression of *Il1rl1* in lymph node-derived immune cells (left) and MACS-sorted sensory
 362 neurons (right) from littermate (LM) control and IL-33R^{Δneuron} mice by RT-qPCR. n > 3
 363 mice/group. (C-G) Assessment of (C) motor activity (rotarod), (D) thermal pain behavior (hot
 364 plate), and acute itch behavior following intradermal injection (i.d.) of (E) histamine, (F)
 365 chloroquine, and (G) serotonin in LM control and IL-33R^{Δneuron} mice. (C-G) n > 4 mice/group (E-
 366 G), 2 combined experiments. Not significant (NS), *p<0.05 by unpaired, two-tailed *t* test.

367
368 **Figure 3: IL-33R signaling in sensory neurons is dispensable for chronic itch in AD-like**
369 **disease.** (A) Schematic of the measurement of IL-33 in the plasma of 11 healthy control (HC)
370 subjects and 11 patients with atopic dermatitis (AD) by Luminex multiplex ELISA. (B) Amount of
371 IL-33 in the plasma of HC subjects and patients with AD. (C) Representative clinical images and
372 H&E sections of ear skin from ethanol (EtOH)- or MC903-treated WT mice (day 12). Scale bar is
373 50 μm . (D) Heatmap and hierarchical clustering of significantly differentially expressed genes in
374 the ear skin of EtOH- or MC903-treated WT mice (day 12). The most differentially expressed
375 genes (1,300 genes) are displayed (based on the t statistic value). $n = 4$ mice/group. Full
376 dataset in Oetjen et al.⁸ (E) Representative clinical images and H&E sections of MC903-treated
377 LM control and IL-33R ^{Δ neuron} mice (day 12). Scale bar is 20 μm . (F) Percent change in ear
378 thickness and (G) number of scratching bouts from MC903-treated LM control and IL-33R ^{Δ neuron}
379 mice over time (days). $n = 13-18$ mice/group (2-3 combined experiments). (B) $*p < 0.05$ by
380 unpaired, two-tailed t test. (F-G) NS by multiple t test using Holm-Sidak method.

381
382 **Figure 4: IL-33 is elevated in CPUO.** Representative clinical images from a patient with (A) AD
383 and (B) chronic pruritus of unknown origin (CPUO). Black boxes indicate zoomed-in view of
384 skin. Representative H&E skin sections from (C) control, (D) patient with AD, and (E) patient
385 with CPUO. Bracket, stratum corneum (SC); brace, epidermis (Epi); black arrow, spongiosis;
386 gray arrow, vascular dilatation; white arrow, dermal perivascular immune infiltrate. Scale bar
387 represents 100 μm . (F) Schematic of the measurement of IL-33 in the plasma of 11 HC subjects
388 (same subjects as in Figure 1) and 8 patients with CPUO by Luminex multiplex ELISA. (G)
389 Amount of IL-33 in the plasma of HC subjects and patients with CPUO. $*p < 0.05$ by unpaired,
390 two-tailed t test.

391

392 **Figure 5: Dry skin itch is dependent on IL-33 signaling in sensory neurons. (A)**
393 Representative clinical images of skin from water- or AEW-treated WT mice (day 5). Frequency
394 of **(B)** immune cells **(C)** mast cells and **(D)** group 2 innate lymphoid cells (ILC2s) in the skin of
395 water- or AEW-treated WT mice (day 5). $n = 6-8$ mice/group (2 combined experiments). **(E)**
396 Number of scratching bouts from water- or AEW-treated WT mice (day 5). $n = 5$ mice/group
397 (representative of 3 experiments). **(F)** Expression of *Il33* by RT-qPCR in water- or AEW-treated
398 skin of WT mice (day 4). $n = 5-7$ mice/group (2 combined experiments). Number of scratching
399 bouts from AEW-treated **(G)** LM control and MastRECK mice, **(H)** control (Cont) and
400 *Rag2/Il2rg*^{-/-} mice, **(I)** LM control and IL-33R^{Δimmune} mice, and **(J)** LM control and IL-33R^{Δneuron}
401 mice (day 5). (G-J) $n = 9-18$ mice/group (2 combined experiments). **(K)** Number of scratching
402 bouts following i.d. injection of Veh or rmlL-33 in WT mice. $n = 6-8$ mice/group (2 combined
403 experiments). **(L)** Representative calcium traces of mouse DRG neurons responding to
404 chloroquine (CQ) after exposure to Veh or rmlL-33. Each trace represents one neuron. **(M)**
405 Percent of CQ-responsive neurons out of all KCl-responsive neurons following exposure to Veh
406 or rmlL-33. $n = >400$ neurons from 3 mice (2 combined experiments). **(B-J, M)** NS, * $p < 0.05$,
407 ** $p < 0.01$, **** $p < 0.0001$ by unpaired, two-tailed *t* test. **(K)** NS by one-way ANOVA with multiple
408 comparisons.

1 **Online Repository**

2

3 **Methods**

4 **Human subjects**

5 Studies were conducted in accordance with The Code of Ethics of the World Medical
6 Association. Written consent was provided by all donors prior to sample collection, and
7 human studies were approved by the Washington University in St. Louis Institutional
8 Review Board. For cytokine profile assessment, blood was collected from patients with
9 moderate-to-severe atopic dermatitis (AD) and chronic pruritus of unknown origin
10 (CPUO) seen by the Division of Dermatology at WUSM/BJH between March 2015 to
11 November 2018 as well as from recruited healthy controls (HCs). Board-certified
12 dermatologists determined the diagnoses of AD based on criteria outlined in Eichenfield
13 et al,^{E1} while the diagnoses of CPUO was based on Kim et al.^{E2} Healthy control and
14 patient demographics are included in **Table E1**. Dorsal root ganglia (DRG) samples
15 were obtained from de-identified US transplant donors under an IRB-exempt protocol at
16 the University of Cincinnati. Control skin sections for H&E were obtained from the skin
17 of patients that presented to the hospital either for an amputation due to chronic ulcers
18 or for cancer resection. There had to be a clear margin for sectioning (at least 10 cm for
19 samples from amputations and 1 cm from tumor resections), which was re-reviewed by
20 a board-certified pathologist.

21

22 **Research animals**

23 All animal experiments were conducted using protocols approved by the Washington
24 University Institutional Animal Care and Use Committee. Mice were maintained in
25 standard husbandry conditions (social housing, 12 hr light-dark cycle, 23°C, food and
26 water *ad libitum*). Wild-type (WT) C56BL/6J were purchased from the Jackson
27 Laboratory. *Rag2/Il2rg*^{-/-} double knockout mice were purchased from Taconic
28 Biosciences. MasTRECK mice were donated by Dr. Seiji Nishino (Stanford University).
29 SNS^{Cre} mice were donated by Dr. Rohini Kuner (Heidelberg University). IL-33R^{flox} were
30 generated by Cyagen Biosciences Inc., California, USA on a C57Bl6/J background. IL-
31 33R^{Δneuron} mice were generated by crossing SNS^{Cre} with IL-33R^{flox} mice. Experiments
32 were conducted with independent cohorts of male and female mice that were 8 -12
33 weeks old except for calcium imaging experiments, where 4-7 week old mice were
34 used. No phenotypic differences based on sex were observed.

35

36 **Chronic itch mouse models**

37 For induction of AD-like disease, the bilateral ear skin of mice (ventral side only) was
38 treated with MC903 (1 nmol in 10 μL of ethanol, Tocris Bioscience) or ethanol (EtOH)
39 control once daily for 12 days as previously described.^{E3} Ear thickness measurements
40 were performed with dial calipers as previously described.^{E4, E5} Percent change was
41 calculated from baseline (day 0).

42

43 To induce dry skin itch, we used the acetone/ether plus water (AEW) model as
44 previously described.^{E6} At least two days prior to the first treatment, we shaved the
45 nape or cheek skin. On treatment days, a 1:1 ratio of acetone (Sigma-Aldrich) + diethyl

46 ether (Sigma-Aldrich) was applied using a cotton pad for 15 seconds to the shaved skin
47 (cheek or nape) followed immediately by application of a cotton pad soaked in distilled
48 water for 30 seconds. Cotton pads used for water treatment were never re-used. Mice
49 received treatments twice daily (~8 hrs apart) for five days.

50

51 **Itch behavior assessment (chronic and acute)**

52 For assessment of itch behavior, mice were acclimated to the test chambers two days
53 prior to the initiation of the experiment. Mice were additionally acclimated for at least 5
54 minutes before each recording. For chronic itch models, we recorded the mice in the
55 morning (before they received any treatment). To assess acute itch responses,
56 acclimated mice were given an intradermal injection of 20 μ L of either histamine (1
57 mg/mL, Sigma-Aldrich), chloroquine (100 μ g, Thermo Fisher Scientific), serotonin (1
58 mM, Sigma-Aldrich), recombinant mouse (rm)IL-33 (50, 300 or 1000 ng; R&D Systems),
59 or saline control into their right cheek (shaved two days prior) and then itch behavior
60 was immediately recorded. Video recordings were manually scored for the number of
61 scratching bouts in a 30-minute period. A scratching bout was defined as a continuous
62 scratching motion by the hindpaw that ended when the mouse placed its paw on the
63 floor or in its mouth. Data for acute itch model only contains cheek-directed scratching
64 bouts (site of pruritogen administration).

65

66 **Pain behavior assessment (thermal sensitivity)**

67 Thermal sensitivity was assessed using the hotplate assay. Hotplate temperature was
68 set to 50°C. Latency was measured as time from mouse being placed on the hotplate

69 and removal upon either flicking/licking of its hind paw or jumping was observed. Data
70 was averaged across two trials taken over two days.

71

72 **Rotarod testing**

73 To test for potential defects in coordinated motor activity, mice were tested using a
74 rotarod system (Ugo Basile) where mice were placed on a rotating treadmill that was
75 accelerated from 5 rotations per minute (rpm) to 40 rpm over 5 minutes (built-in program
76 of the apparatus). Time was recorded from acceleration initiation until mice fell from the
77 rod or completed one passive rotation (time to failure). Training occurred over 3 days
78 prior to testing day with 3 trials conducted per day with a 10-minute break between each
79 trial. On testing day, 3 trials were completed with a 10-minute break between each trial
80 and data was averaged across all trials.

81

82 **Basophil and mast cell depletion**

83 Basophil and mast cell depletion was performed as previously described.^{E7} Briefly,
84 MastRECK and littermate (LM) mice were treated daily with intraperitoneal (i.p.)
85 injections of diphtheria toxin (DT; 250 ng in 100 μ L of PBS; Sigma-Aldrich) for five
86 consecutive days immediately prior to initiation of AEW treatments. Depletion was
87 verified by flow cytometry (**Fig E2**).

88

89 **Histological analysis**

90 To assess murine AD-like histopathology, ears were harvested from EtOH- or MC903-
91 treated mice and were fixed in 4% paraformaldehyde (PFA, Thermo Fisher Scientific),

92 embedded in paraffin, sectioned, and stained with hematoxylin and eosin (H&E).
93 Histology for Fig 3, C was performed by WUSM Digestive Disease Research Core
94 Center and slides were imaged using the NanoZoomer 2.0-HT System (Hamatsu).
95 Histology for Fig 3, E was performed by HistoWiz Inc (histowiz.com) using a standard
96 operating procedure and fully automated workflow. For human histopathology, 4 mm
97 punch biopsies of human skin were collected and fixed in 10% PFA. Samples were
98 embedded in paraffin and sections were stained with H&E. Slides were imaged using
99 the NanoZoomer 2.0-HT System (Hamatsu).

100

101 **Plasma cytokine measurement**

102 IL-33 levels in human samples were assessed using a custom Luminex ELISA kit (R&D
103 Systems) as previously described.^{E8} Plasma was isolated following Ficoll gradient
104 separation of peripheral blood drawn from patients with AD, patients with CPUO, or
105 healthy control subjects (**Table E1**). Before the detection assay, plasma was diluted (1:1
106 in assay diluent), loaded onto Protein L-coated plates (Thermo Fisher Scientific), and
107 incubated on an orbital shaker at room temperature for 90 minutes. FLEXMAP three-
108 dimensional system (Thermo Fisher Scientific) was used to collect the data.

109

110 **RNA-seq data analysis**

111 We reanalyzed RNA-seq data of mouse ear skin treated with MC903 or EtOH (in Fig 3,
112 D). Dataset was obtained from NCBI GEO^{E9} under the accession number GSE90883.
113 Full methods on sample processing are available in Oetjen et al.^{E3} For our re-analysis,
114 duplicate genes were removed, and genes were filtered for protein coding designation.
115 Using row mean (counts), the top 12,000 genes were selected for additional

116 downstream analysis. Differential gene expression was calculated using the *limma* R
117 package with the online Phantasus software (<https://artyomovlab.wustl.edu/phantasus/>)
118 along with hierarchical clustering (one minus pearson correlation) and heatmap
119 generation. Only top 1,300 most differentially expressed genes are displayed in figure
120 (based on *t* value).

121

122 **Single cell RNA-seq data analysis**

123 We reanalyzed single cell RNA-sequencing dataset of mouse dorsal root ganglia (in Fig.
124 1, I-K). Dataset was obtained from NCBI GEO^{E9} under the accession number
125 GSE158892. Full methods on sample processing are available in Avraham et al.^{E10}
126 Data analysis and processing was performed using commercial code from Partek Flow
127 package at <https://www.partek.com/partek-flow/>. Processed data are publicly available
128 at <https://mouse-drg-injury.cells.ucsc.edu/>.

129

130 **Mouse RNA isolation and qRT-PCR**

131 For RNA isolation from the whole dorsal root ganglia (DRG), DRG were harvested from
132 naïve wild-type (WT) mice and homogenized in 1 mL Trizol Reagent (Life Technologies)
133 with a bead homogenizer (BioSpec). RNA was extracted using the RNeasy Mini Kit
134 (QIAGEN) and DNA was digested using Turbo DNA-free Kit (Invitrogen) following the
135 manufacturer's instructions.

136

137 For RNA isolation from purified DRG neurons, DRG were harvested from LM control
138 and IL-33R^{Δneuron} mice then digested as previously described.^{E3,E11} Briefly, DRG was

139 incubated in $\text{Ca}^{2+}/\text{Mg}^{2+}$ -free HBSS containing collagenase type I (342 U/mL; GIBCO)
140 and dispase II (3.8 U/mL; GIBCO) at 37°C on a rotator for 30-40 minutes. Sample was
141 triturated then transferred into MACS buffer (0.5% BSA in DPBS). Sensory neurons
142 were negatively selected from the DRG using the MACS Neuron Isolation kit (130-115-
143 389; Miltenyi Biotec) as previously described by Thakur et al.^{E12} RNA was extracted
144 using the Nucleospin RNA XS kit (Takara Bio) according to manufacturer's instructions.

145
146 For RNA isolation from immune cells, lymph nodes were harvested (inguinal,
147 mesenteric, and superficial cervical) from naïve LM control and IL-33R^{Δneuron} mice
148 before being manually homogenized through a 70 μm cell strainer and washed (5%
149 FBS in DMEM). RNA was extracted using the Nucleospin RNA kit (Takara Bio)
150 according to manufacturer's instructions.

151
152 For RNA isolation from skin, water control- or AEW-treated cheek skin from WT mice
153 were harvested 4 hours following the last treatment of AEW on day 4 of AEW mouse
154 model. Skin samples were stored in RNAlater (Invitrogen) at 4°C before transfer to -
155 80°C. Following tissue homogenization with a bead homogenizer (BioSpec) in 350 μL of
156 RNA lysis buffer (Nucleospin RNA, Takara Bio), RNA was isolated using the Nucleospin
157 RNA kit (Takara Bio) per the manufacturer's instructions.

158
159 Following all upstream protocols of RNA isolation, cDNA was synthesized using the
160 High-Capacity cDNA Reverse Transcription Kit (Applied Biosystems). For relative
161 quantification of *I/33* mRNA, qRT-PCR was performed with 10 ng of cDNA, pre-

162 validated commercial primers (Mm.PT.58.31135215; Integrated DNA Technologies),
163 and the Fast SYBER Green Master Mix (Applied Biosystems) on a StepOnePlus
164 machine (Applied Biosystems). For relative quantification of *Il1rl1* mRNA, qRT-PCR was
165 performed with 10 ng of cDNA, pre-validated commercial primer-probe assay
166 (Mm.PT.58.11610831.g; Integrated DNA Technologies), and the TaqMan Gene
167 Expression Master Mix (Applied Biosystems) on a StepOnePlus machine (Applied
168 Biosystems). Gene expression was normalized to *Gapdh* (Mm.PT.39a.1; Integrated
169 DNA Technologies). Fold change was calculated using the $2^{-\Delta\Delta CT}$ method.^{E13} Products
170 from *Il1rl1* qRT-PCR reaction were run on a 2% agarose gel with 1 mg/mL of ethidium
171 bromide at 140 V.

172

173 **Human RNA isolation and RT-PCR**

174 Human dorsal root ganglia (hDRG) were dissected from donors and the fat, dura, and
175 connective tissues were removed as previously described.^{E14} Samples were kept in
176 RNAlater (Sigma-Aldrich) at -80°C. One half of a single DRG was homogenized in 1 mL
177 of Trizol Reagent according to manufacturer's instructions for total RNA extraction. For
178 genomic DNA elimination and cDNA synthesis, the Maxima H Minus First Strand cDNA
179 Synthesis Kit with dsDNase (Thermo Scientific) was used with the *IL1RL1* primer set
180 (Forward: CAG GGA GCG GCA GGA ATG T, Reverse: CTT GCA TTT ATC AGC CTC
181 CAG AGA A; Millipore Sigma) in accordance with manufacturer's instructions. For gel
182 electrophoresis, RT-PCR product was loaded onto a 2% agarose gel with 1 mg/mL of
183 ethidium bromide at 100 V.

184

185 Calcium imaging of mouse DRG neurons

186 We isolated mouse DRG neurons and performed calcium imaging as previously
187 described.^{E3,11} Following euthanasia via CO₂ inhalation, the DRG were harvested.
188 Nerve fibers were trimmed, and connective tissue was removed from the DRGs. For
189 enzymatic dissociation, DRGs were incubated in 1 mL of Ca²⁺/Mg²⁺-free HBSS
190 containing collagenase type I (342 U/mL; Worthington Biochemical Corporation) and
191 dispase II (4 U/mL; GIBCO) at 37°C on a rotator for 30 - 40 minutes. DRGs were then
192 triturated to generate a single cell suspension. Dissociated DRG neurons were then
193 seeded on 8 mm glass pre-coated with poly-D-lysine (20 mg/mL, Fisher) and laminin
194 (20 mg/mL, Sigma). Cells were cultured overnight at 37°C with 5% CO₂ in Neurobasal-A
195 culture medium (GIBCO) supplemented with nerve growth factor (100 ng/mL; Sigma-
196 Aldrich), glial cell-derived neurotrophic factor (20 ng/mL; Sigma-Aldrich), B-27 (2%;
197 GIBCO), penicillin (100 U/mL; Sigma-Aldrich), streptomycin (100 mg/mL; Sigma-
198 Aldrich), and 10% FBS (Sigma-Aldrich).

199
200 The following day, the cultured DRG neurons were loaded with the calcium indicator
201 dye Fura-2 AM (4 μM; Invitrogen) for 20-45 min then washed with calcium imaging
202 buffer (130 mM NaCl, 3 mM KCl, 2.5 mM CaCl₂, 0.6 mM MgCl₂, 10 mM HEPES, 10 mM
203 glucose, 1.2 mM NaHCO₃). Slides were imaged with alternating 340 and 380 nm
204 excitation wavelengths using an inverted Nikon Ti-S microscope, CoolSNAP CCD
205 camera (Photometrics), and NIS-elements software (Nikon Instruments). Capsaicin (300
206 nM; Sigma-Aldrich), histamine (50 μM, Sigma-Aldrich), and KCl (100 mM; Sigma-
207 Aldrich) were applied to DRG neurons via perfusion. rmlL-33 (1 μg/mL; R&D Systems)

208 and vehicle control (0.1% BSA (Sigma-Aldrich) in PBS) were manually loaded by gently
209 pipetting the solution into the recording chamber. Cells were washed with calcium
210 imaging buffer for at least 3 minutes between stimuli. For sensitization experiments, we
211 evaluated the response of DRG neurons to chloroquine (1 mM; MP Biomedicals)
212 immediately after stimulation with vehicle control (0.1% BSA) or rmlL-33 (4 µg/mL) with
213 no wash between exposure to vehicle or rmlL-33 and chloroquine. Fluorescence ratios
214 (340/380) were normalized to baseline. A change in the fluorescence ratio (340/380) of
215 greater than 10% was considered to be a cellular response.

216

217 **Calcium imaging of human DRG neurons**

218 We isolated human DRG neurons and performed calcium imaging as previously
219 described^{E3,14}. Following DRG dissociation, cells were plated on glass coverslips and
220 incubated for 3 days in Neurobasal-A media supplemented with B-27, penicillin (100
221 U/mL) plus streptomycin, Glutamax (2 mM; GIBCO) and FBS (5%) at 37°C with 5%
222 CO₂. Cells were loaded with Fura-2 AM (3 µg in 3 µL DMSO in 1 mL of media) before
223 imaging on an Olympus BX51 microscope with Rolera Bolt camera (Q-Imaging) and a
224 CoolLED pE-4000 (365/385) illumination system controlled via MetaFluor software
225 (Molecular Devices). Recombinant human IL-33 (1 µg/mL; R&D Systems), capsaicin
226 (250 nM) and KCl (60 mM) were administered to the bath. A change in the fluorescence
227 ratio (340/380) of greater than 10% was considered to be a cellular response.

228

229 **Flow cytometry**

230 Samples were collected on day 5 of the AEW mouse model. For skin digestion, tissue
231 was minced then incubated in 500 μ L of Liberase TL (0.25 mg/mL; Roche) in DMEM
232 (Sigma-Aldrich) at 37°C and 5% CO₂ for 90 min. To obtain a single-cell suspension,
233 skin and spleen samples were then manually homogenized through a 100 μ m cell
234 strainer. To lyse erythrocytes in spleen samples, samples were resuspended in 2 mL of
235 Red Blood Cell Lysis Buffer Hybri-Max (Sigma-Aldrich) and incubated for 5 min. To test
236 for cellular viability, all cells were stained with Zombie UV dye (1:500; Biolegend) for 20
237 minutes at room temperature. Blocking solution (anti-mouse CD16/CD32 - 2.4G2 clone;
238 2 μ g/mL; Bio X Cell) was applied to cells for 10 min (4°C) before cells were stained with
239 primary antibodies diluted in BD Horizon Brilliant Stain Buffer for 30 min (4°C). Cells
240 were then stained with secondary streptavidin-conjugated antibodies for 15 min (4°C).
241 Finally, cells were fixed overnight at 4°C with BD Cytoperm/Cytofix reagent before
242 sample acquisition on a LSR Fortessa X-20 (BD Biosciences). Data were analyzed with
243 FlowJo 10 (Tree Star). Immune cells were defined as live CD45⁺ cells.

244

245 Group 2 innate lymphoid cells (ILC2s) were defined as live IL7R⁺ KLRG1⁺ ST2⁺ cells
246 that were negative for the lineage (Lin) markers: CD11b, CD11c, NK1.1, CD19, Fc ϵ R1 α ,
247 CD3 ϵ , and CD4. Thus, cells were stained with the following antibodies to determine
248 ILC2 frequencies: CD11b PerCP/Cy5.5 (M1/70; eBioscience), CD11c PerCP/Cy5.5
249 (N418; eBioscience), NK1.1 PerCP/Cy5.5 (PK136; eBioscience), CD19 PerCP/Cy5.5
250 (1D3; eBioscience), Fc ϵ R1 α PerCP/Cy5.5 (MAR-1; Biolegend), CD3 ϵ Pe/Cy7 (145-
251 2C11; Biolegend), CD4 BV421 (GK1.5; Biolegend), IL7R α (CD127) BV650 (A7R34;

252 Biolegend), KLRG1 PE/Daz (MAFA; Biolegend), ST2 Biotin (RMST2-2; eBioscience),
253 and Streptavidin FITC (Biolegend).

254

255 Basophils were defined as live $Fc\epsilon R1\alpha/IgE^+$ $CD49b^+$ cells that were negative for c-KIT,
256 Siglec-F and the Lin markers: CD5, CD11c, CD19, and NK1.1. Mast cells were defined
257 as live c-KIT⁺ $Fc\epsilon R1\alpha/IgE^+$ cells that were negative for SiglecF and the Lin markers:
258 CD5 or CD3 ϵ , CD11c, CD19, and NK1.1. Thus, cells were stained with the following
259 antibodies to evaluate basophil and mast cell frequencies: CD5 PerCP/Cy5.5 (53-7.3;
260 eBioscience) or CD3e PerCP/Cy5.5 (145-2C11; eBioscience), CD11c PerCP/Cy5.5
261 (N418; eBioscience), CD19 PerCP/Cy5.5 (1D3; eBioscience), NK1.1 PerCP/Cy5.5
262 (PK136; eBioscience), Siglec-F BV421 (E50-2440; BD Bioscience), c-KIT (CD117)
263 Pe/Cy7 (2B8, eBioscience) or c-KIT BV605 (ACK2; Biolegend), $Fc\epsilon R1\alpha$ FITC (MAR-1;
264 eBioscience), IgE FITC (23G3; eBioscience), and CD49b APC (DX5; eBioscience).

265

266 **Statistical analysis**

267 All data are presented as mean \pm standard deviation. Data from independent
268 experiments were pooled where indicated. Statistical significance for two groups were
269 determined using a two-tailed, unpaired Student's *t* test or multiple *t* test using Holm-
270 Sidak method. Differences were considered significant if $p < 0.05$. Venn diagrams were
271 generated using BioVenn.^{E15} Graphical results and statistical testing for RNA-seq were
272 conducted using Phantasus (<https://artyomovlab.wustl.edu/phantasus/>). scRNAseq
273 analysis was generated using Partek Flow package ([https://www.partek.com/partek-](https://www.partek.com/partek-flow/)
274 [flow/](https://www.partek.com/partek-flow/)). Outliers were identified based on the ROUT method (Q = 1%; GraphPad Prism7

275 Software). The remainder of graphs were generated and statistical analysis were
276 preformed using GraphPad Prism7 Software. Significance is labeled as: N.S., not
277 significant, * $p < 0.05$, ** $p < 0.01$, **** $p < 0.0001$.

278

279 **References**

- 280 E1. Sidbury R, Wynn TL, Bergman JN, Cooper KD, Silverman RA, Berger TG, et al.
281 Guidelines of care for the management of atopic dermatitis. *J Am Acad Dermatol.*
282 2014;71:1218–33.
- 283 E2. Kim BS, Berger TG, Yosipovitch G. Chronic pruritus of unknown origin (CPUO):
284 Uniform nomenclature and diagnosis as a pathway to standardized understanding
285 and treatment. *J Am Acad Dermatol.* 2019;81:1223–4.
- 286 E3. Oetjen LK, Mack MR, Feng J, Whelan TM, Niu H, Guo CJ, et al. Sensory Neurons
287 Co-opt Classical Immune Signaling Pathways to Mediate Chronic Itch. *Cell.*
288 2017;171:217-228.e13.
- 289 E4. Kim BS, Siracusa MC, Saenz SA, Noti M, Monticelli LA, Sonnenberg GF, et al.
290 TSLP elicits IL-33-independent innate lymphoid cell responses To Promote Skin
291 Inflammation. *Sci Transl Med.* 2013;5:170ra16.
- 292 E5. Kim BS, Wang K, Sircusa MC, Saenz SA, Brestoff JR, Monticelli LA, et al.
293 Basophils Promote Innate Lymphoid Cell Responses in Inflamed Skin. *J Immunol.*
294 2014;193:3717–25.
- 295 E6. Miyamoto T, Nojima H, Shinkado T, Nakahashi T, Kuraishi Y. Itch-Associated
296 Response Induced by Experimental Dry Skin in Mice. *Jpn J Pharmacol.*
297 2002;88:285–92.
- 298 E7. Otsuka A, Kubo M, Honda T, Egawa G, Nakajima S, Tanizaki H, et al.
299 Requirement of interaction between mast cells and skin dendritic cells to establish
300 contact hypersensitivity. *PLoS One.* 2011;6:e25538.
- 301 E8. Mack MR, Brestoff JR, Berrien-Elliott MM, Trier AM, Yang TLB, McCullen M, et al.
302 Blood natural killer cell deficiency reveals an immunotherapy strategy for atopic
303 dermatitis. *Sci Transl Med.* 2020;12:eaay1005.
- 304 E9. Barrett T, Wilhite SE, Ledoux P, Evangelista C, Kim IF, Tomashevsky M, et al.
305 NCBI GEO: Archive for functional genomics data sets - Update. *Nucleic Acids*
306 *Res.* 2013;41:991–5.
- 307 E10. Avraham O, Feng R, Ewan EE, Zhao G, Cavalli V. Profiling sensory neuron
308 microenvironment after peripheral and central axon injury reveals key pathways
309 for axon regeneration. *bioRxiv.* 2020; doi: 10.1101/2020.11.25.398537
- 310 E11. Wang F, Trier AM, Li F, Kim S, Chen Z, Chai JN, et al. A basophil-neuronal axis
311 promotes itch. *Cell.* 2021;184:422-440.e17.
- 312 E12. Thakur M, Crow M, Richards N, Davey GIJ, Levine E, Kelleher JH, et al. Defining
313 the nociceptor transcriptome. *Front Mol Neurosci.* 2014;7:87.
- 314 E13. Livak KJ, Schmittgen TD. Analysis of relative gene expression data using real-
315 time quantitative PCR and the 2- $\Delta\Delta$ CT method. *Methods.* 2001;25:402–8.
- 316 E14. Valtcheva M, Samineni V, Golden J, Gereau R, Davidson S. Enhanced non-
317 peptidergic intraepidermal fiber density and an expanded subset of chloroquine-

318 responsive trigeminal neurons in a mouse model of dry skin itch. *J Pain*.
 319 2015;16:346–56.
 320 E15. Hulsén T, de Vlieg J, Alkema W. BioVenn - A web application for the comparison
 321 and visualization of biological lists using area-proportional Venn diagrams. *BMC*
 322 *Genomics*. 2008;9:488.
 323
 324

Characteristic	Control	AD	CPUO
Subjects (N)	11	11	8
Mean age (yr)	37.1 ± 12.6	43.7 ± 15.0	77.8 ± 5.3
Percent female	54.5%	45.5%	12.5%

325
 326 **Table E1: Demographics for subjects analyzed in Fig. 2 & 3, plasma cytokines.**

327 Data are represented as mean ± SD.

328

329 **Figure E1: Mouse models of chronic itch.** (A) Schematic of treatment course for
 330 inducing AD-like disease. Mice are treated once daily for 12 days with ethanol (EtOH) or
 331 MC903. (B) Schematic of treatment course for inducing dry skin itch, a model that
 332 mirrors CPUO. Mice are treated twice daily for 5 days with water-only control or AEW
 333 (acetone/ether plus water).

334

335 **Figure E2: Depletion of mast cells and basophils following DT treatment in**
 336 **MasTRECK mice.** (A) Schematic of selective depletion of mast cells and basophils.
 337 Littermate (LM) control and MasTRECK mice received daily intraperitoneal (i.p.)
 338 injections of diphtheria toxin (DT) for five days prior to the initiation of AEW treatment.
 339 (B) Representative flow cytometry plots and frequency of mast cells in the skin of AEW-
 340 treated LM control and MasTRECK mice (day 5). n = 5-9 mice/group. Representative
 341 flow cytometry plots and frequency of basophils (C) in the spleen and (D) the skin of
 342 AEW-treated LM control and MasTRECK mice (day 5). n = 5-9 mice/group. Data are

343 representative of two independent experiments. Unpaired, two-tailed t test was used for
344 all statistical analyses. NS, **** $p < 0.0001$ by unpaired, two-tailed t test.

Journal Pre-proof

Figure 1: Mouse and human DRG express IL-33R

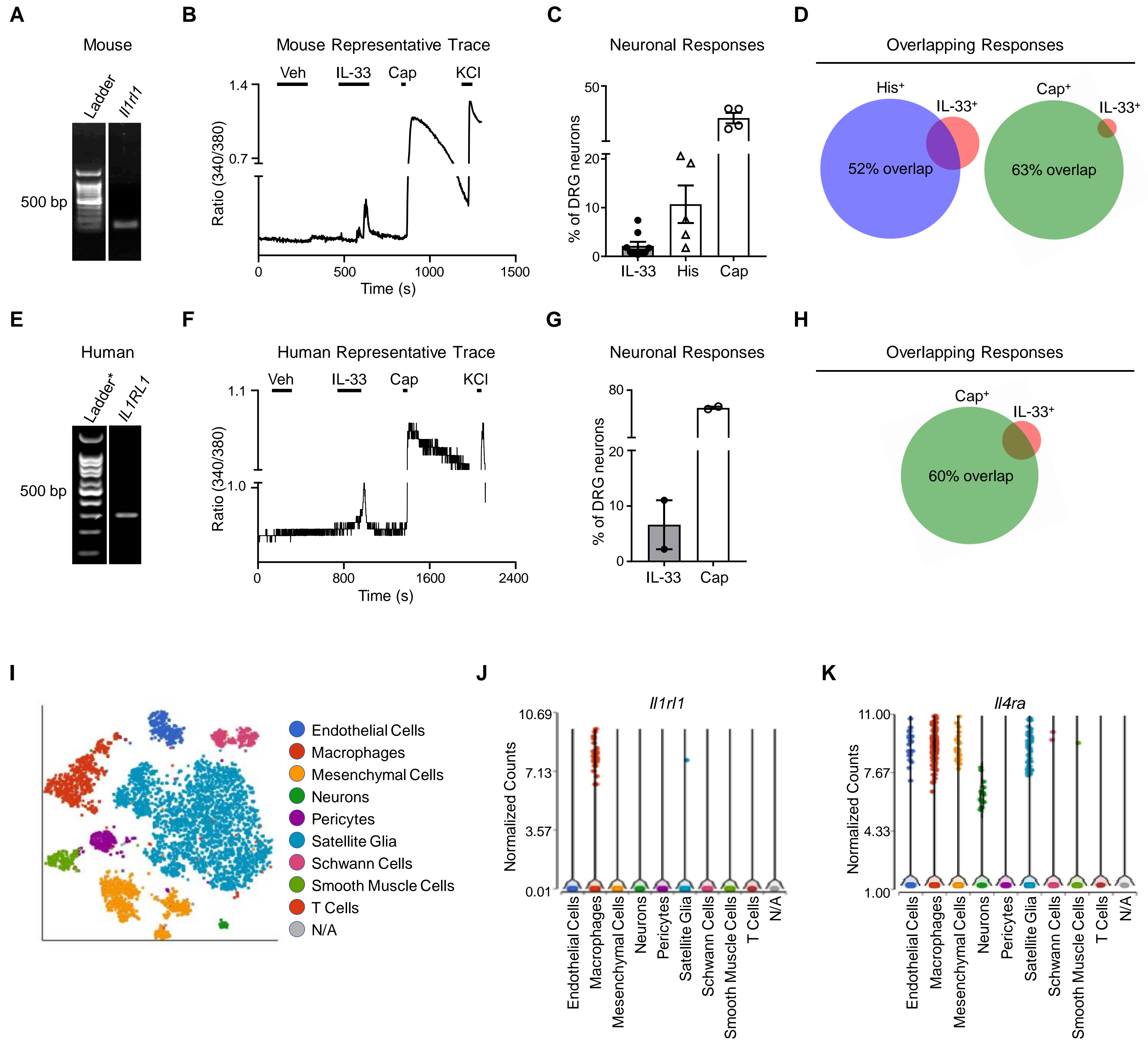
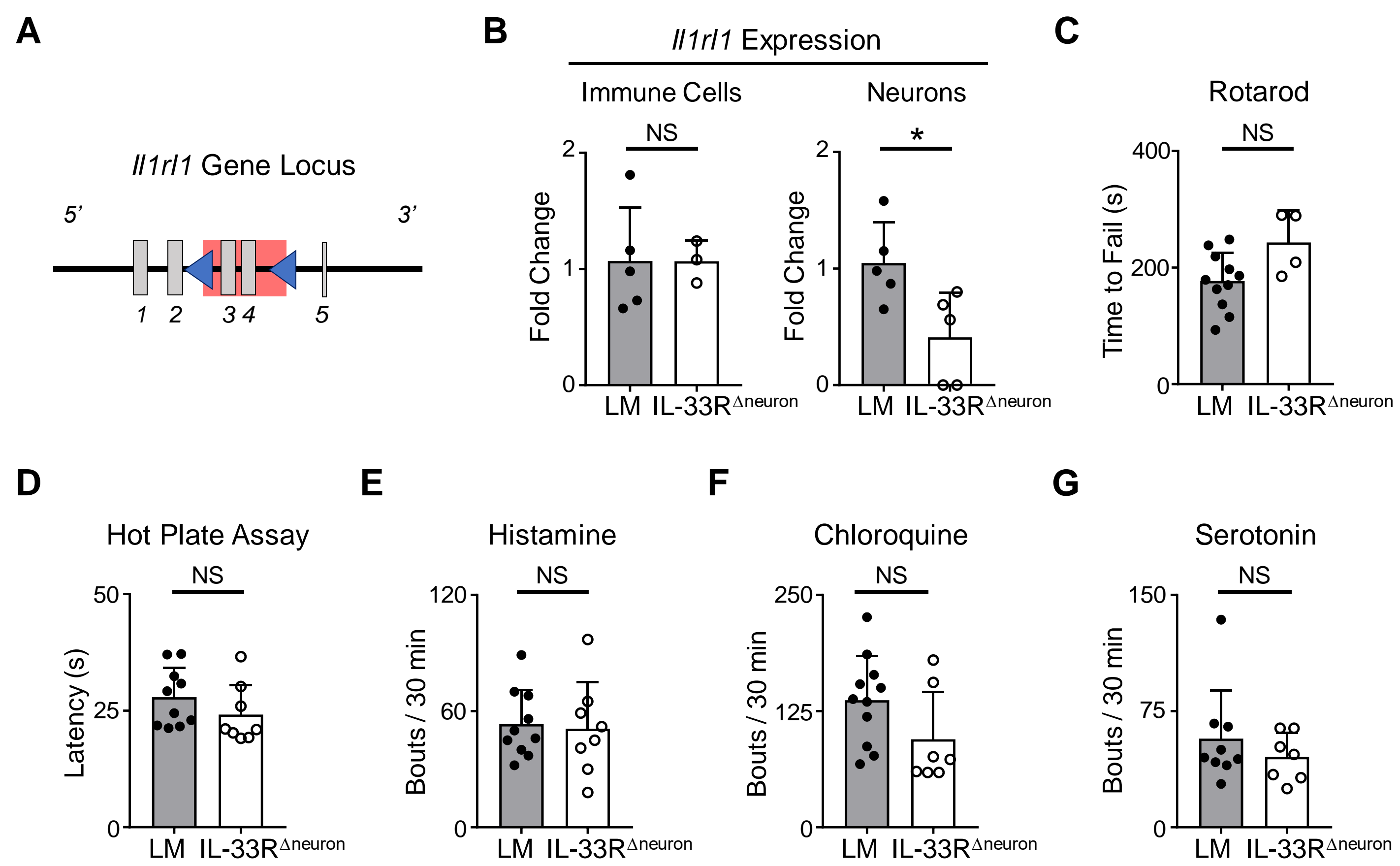


Figure 2: Generation of novel conditional IL-33R knock-out mice



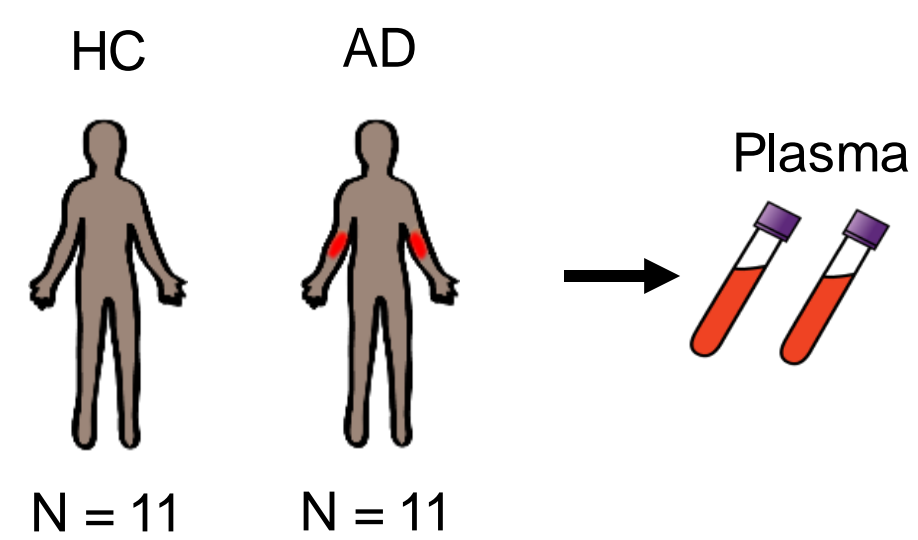
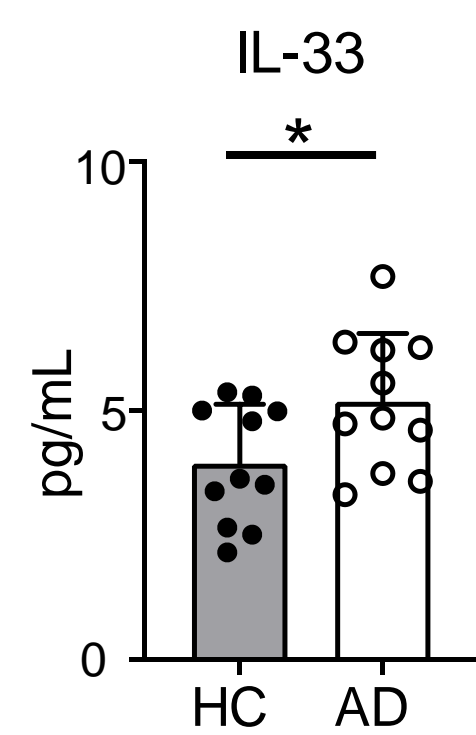
A**B**

Figure 3: IL-33R signaling in sensory neurons is dispensable for chronic itch in AD-like disease

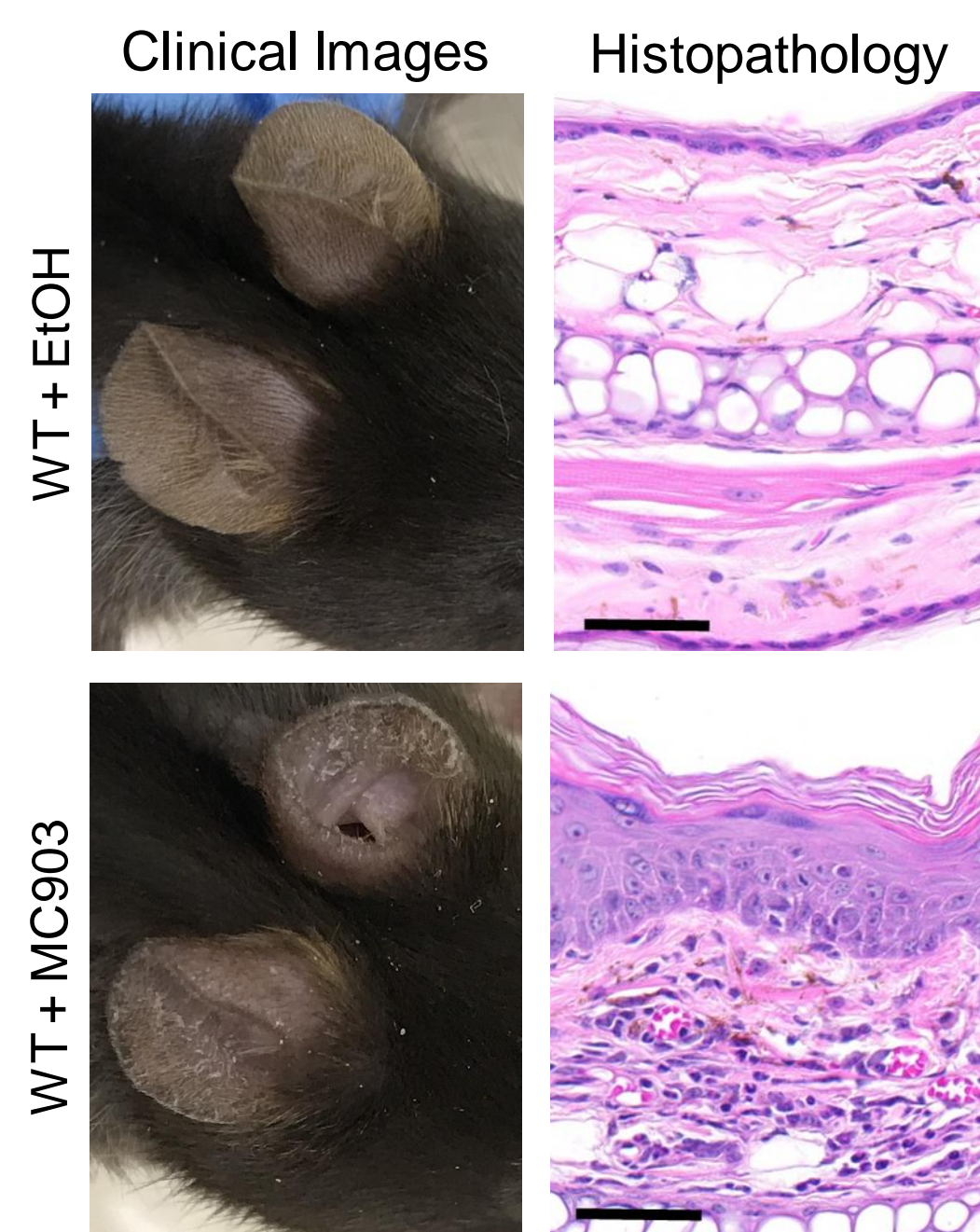
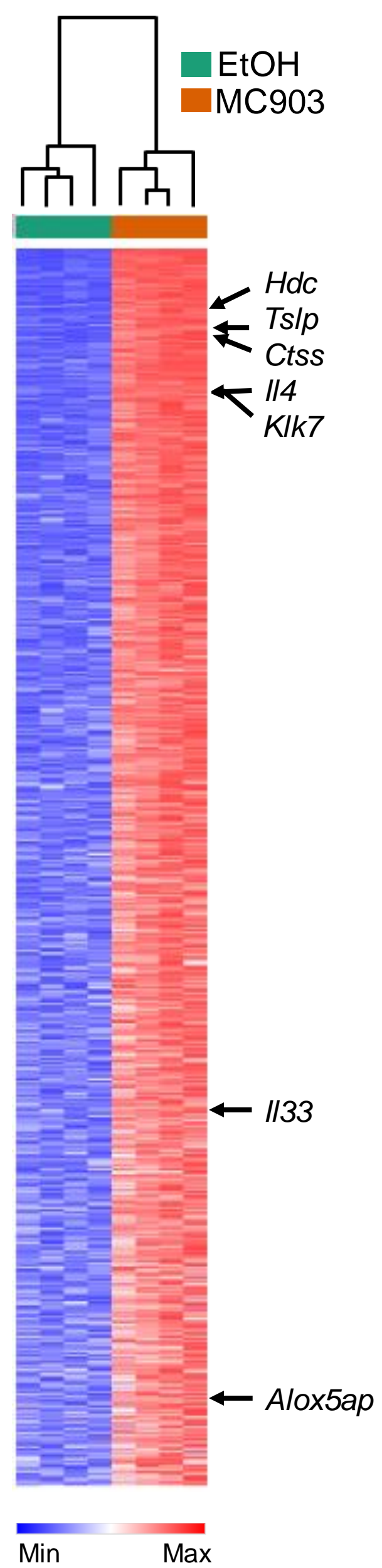
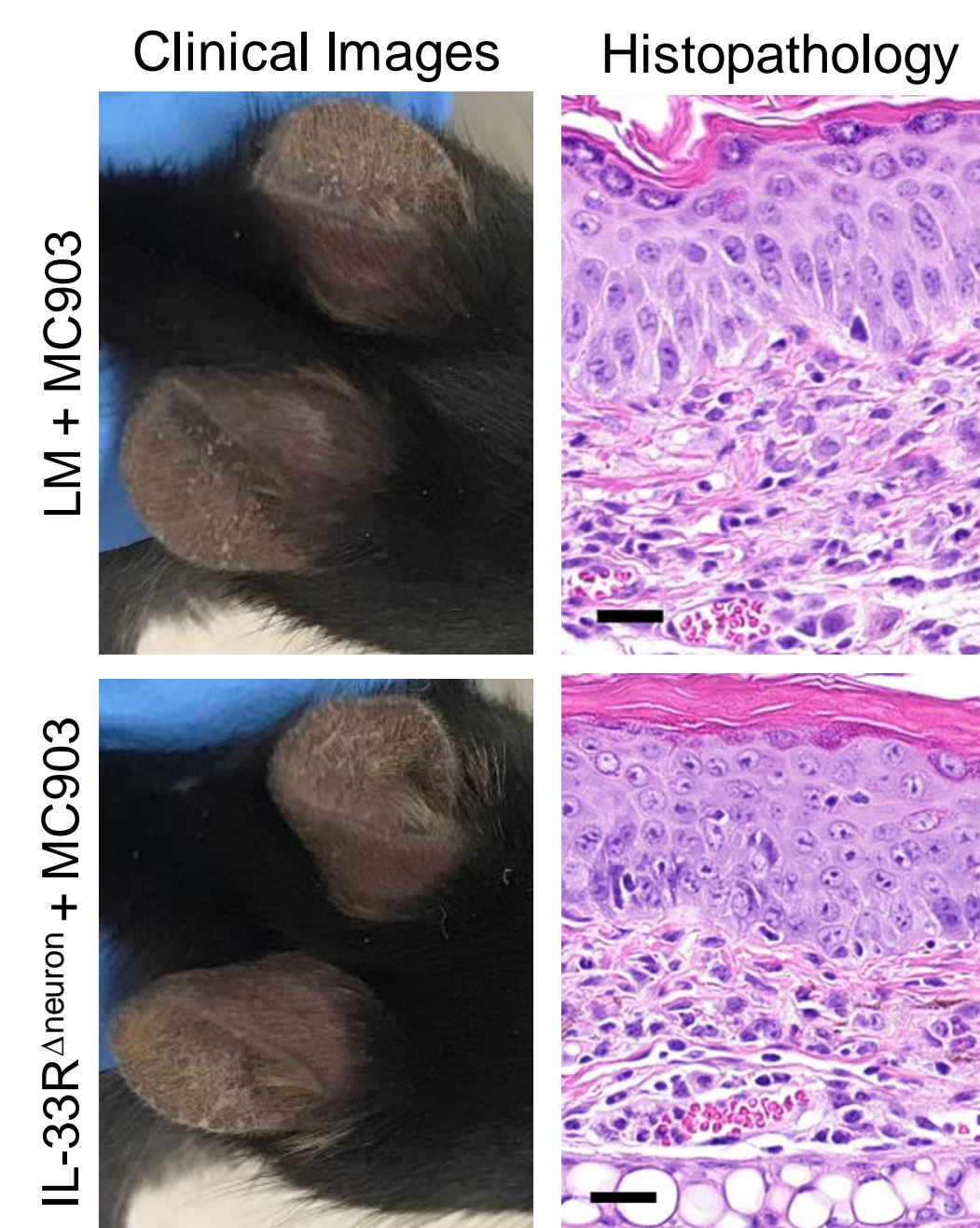
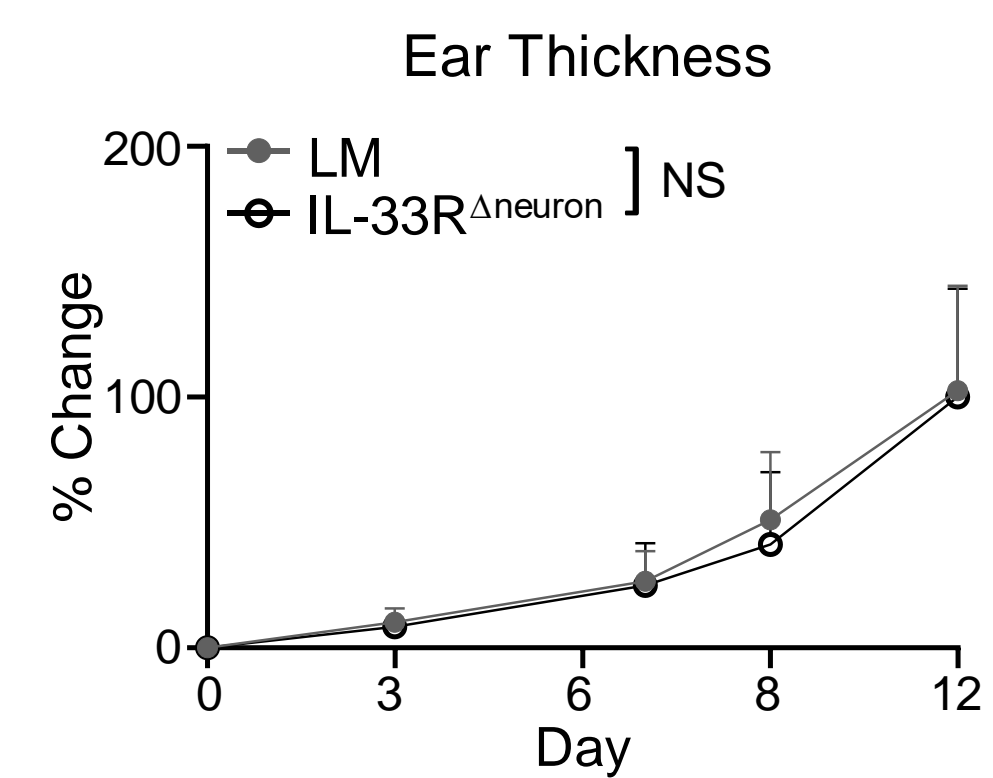
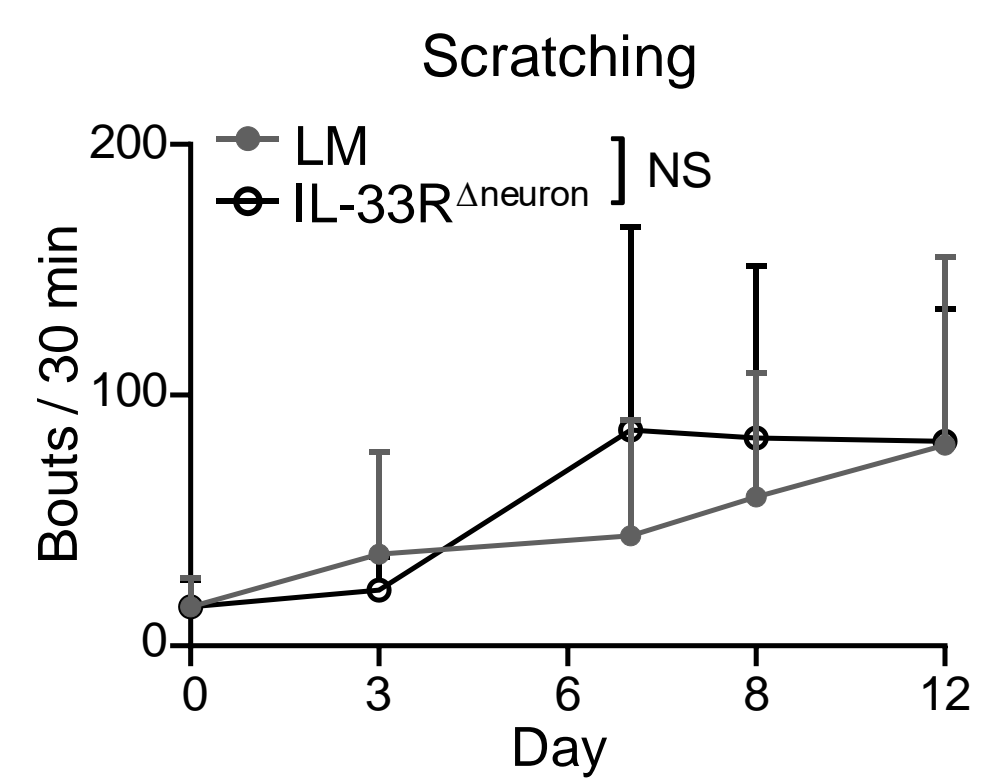
C**D****E****F****G**

Figure 4: IL-33 is elevated in CPUO

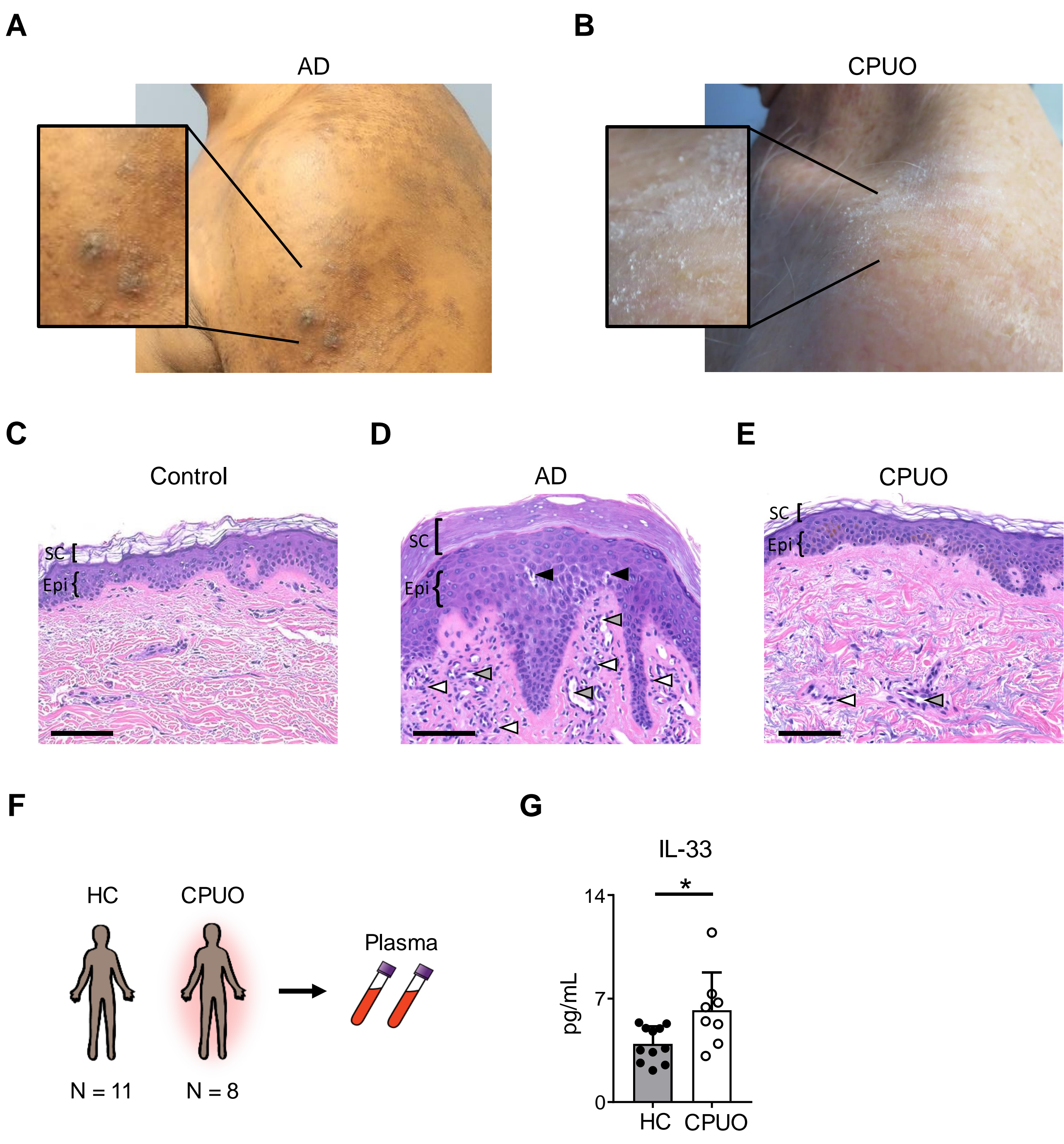


Figure 5: Dry skin itch is dependent on IL-33 signaling in sensory neurons

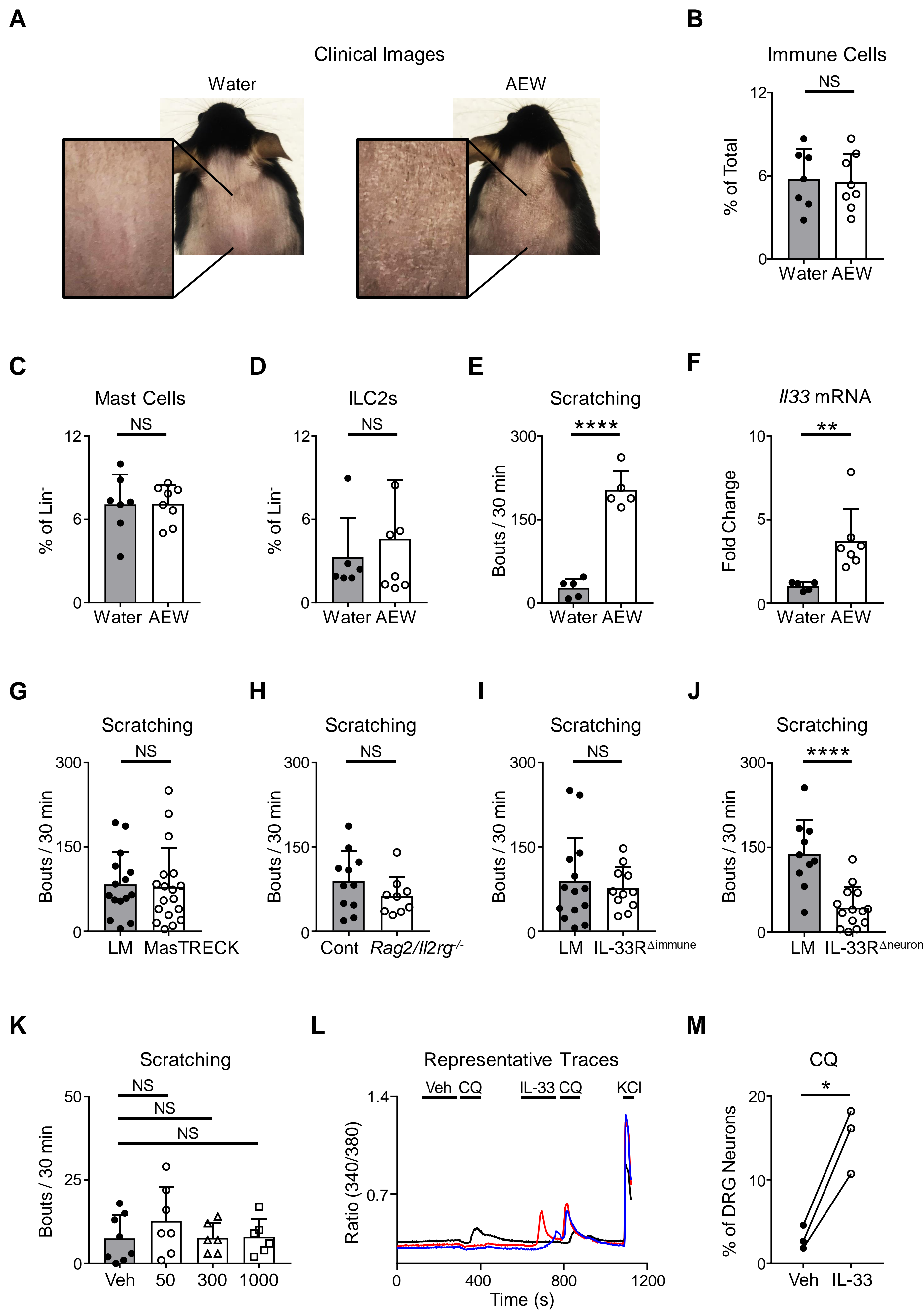
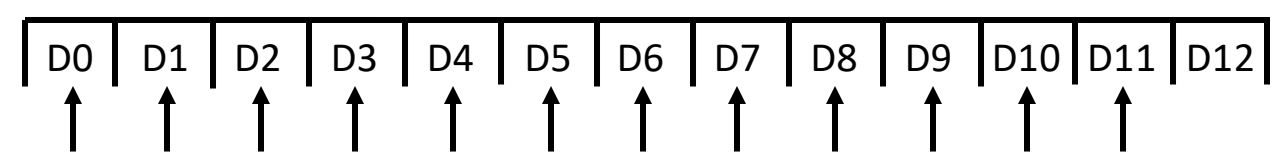


Figure E1: Mouse models of chronic itch

A

MC903 Model



EtOH

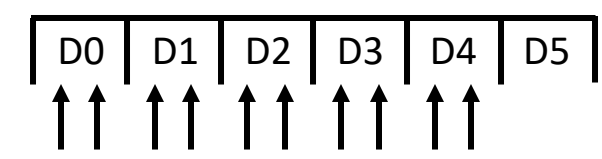


MC903



B

Acetone / Ether + Water Model



Water

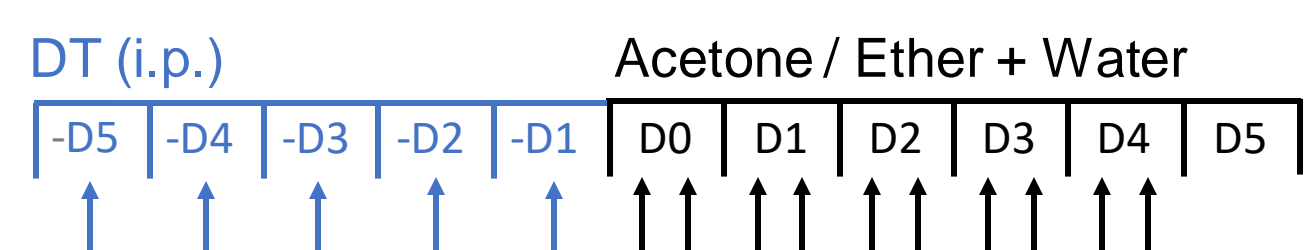


AEW

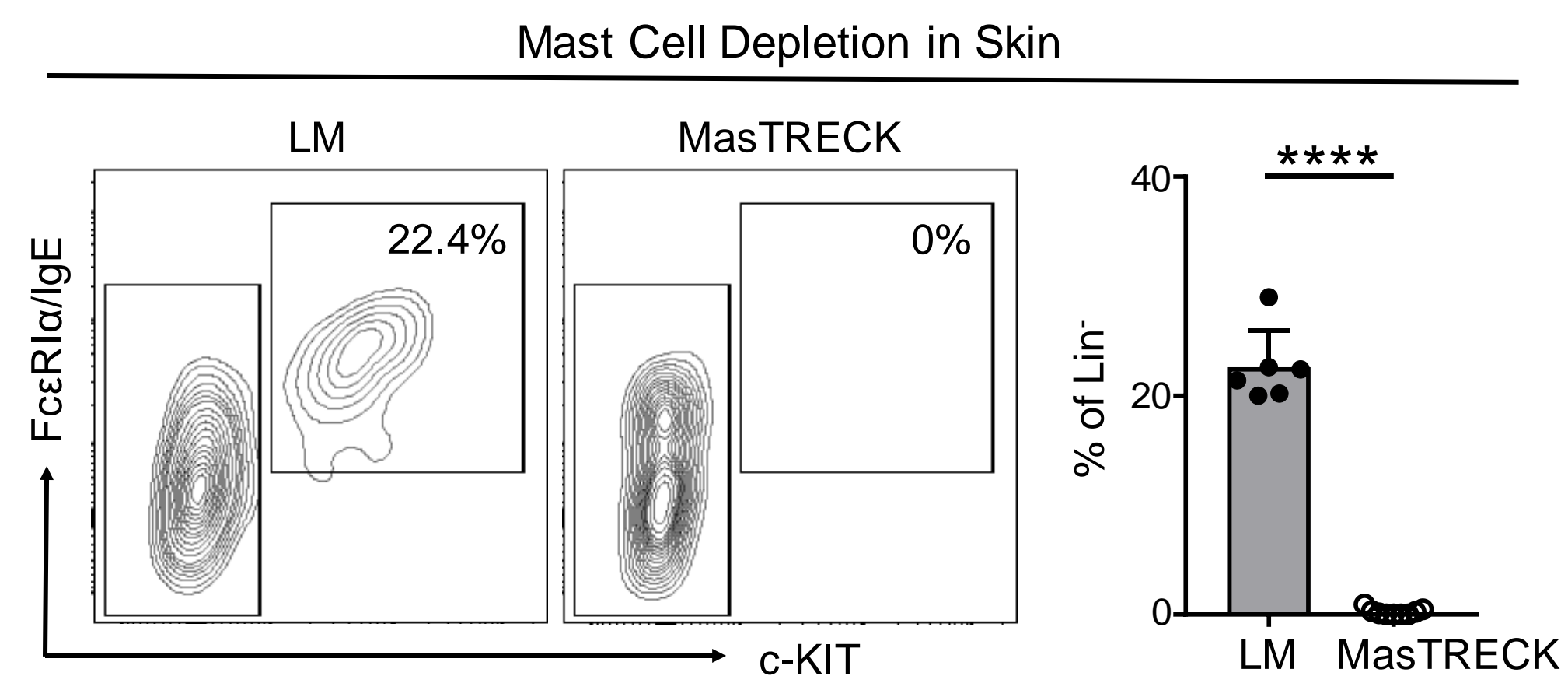


Figure E2: Depletion of mast cells and basophils following DT treatment in MastTRECK mice

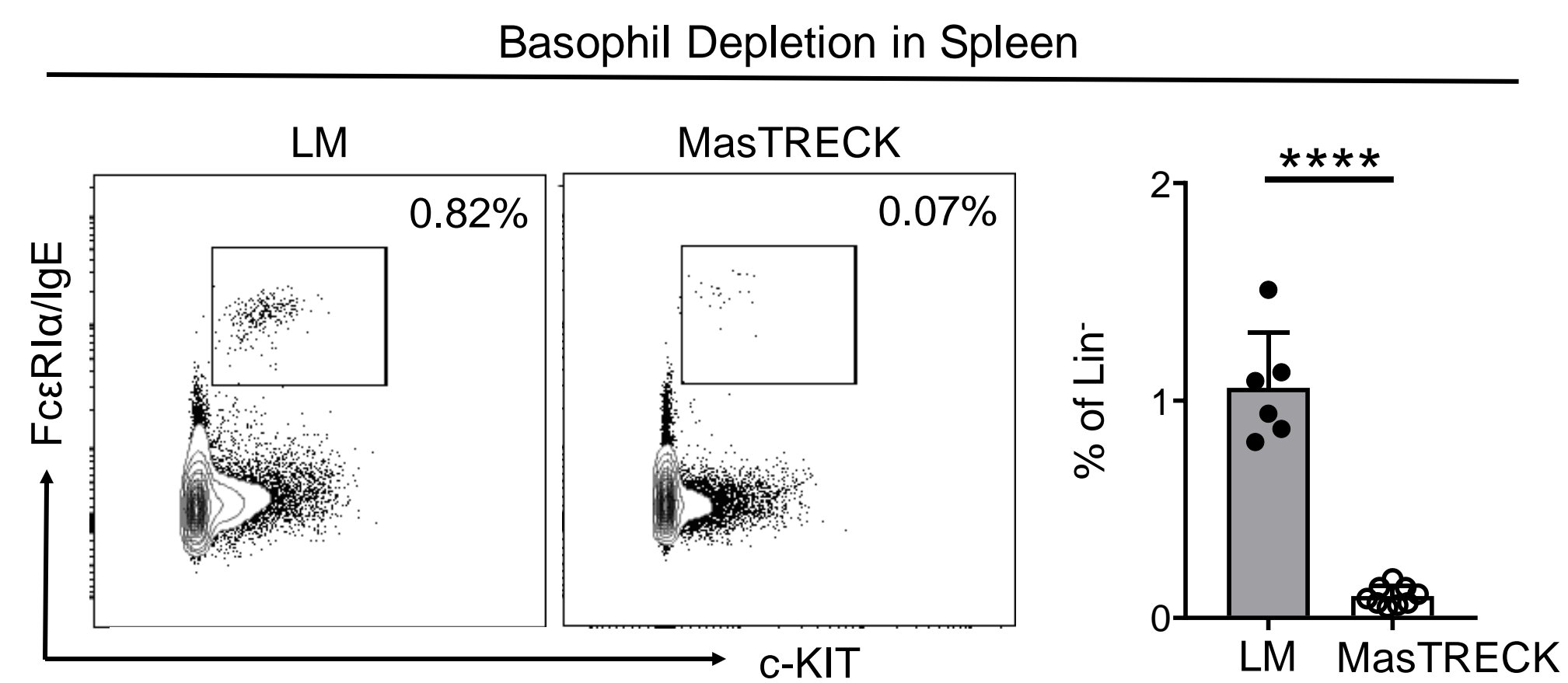
A



B



C



D

